Geologica Acta, Vol.4, Nº1-2, 2006, 103-121
Available online at www.geologica-acta.com

geologica acta

Primitive Cretaceous island-arc volcanic rocks in eastern Cuba: the Téneme Formation

J.A. PROENZA [1] R. DÍAZ-MARTÍNEZ [2] A. IRIONDO [3] C. MARCHESI [4] J.C. MELGAREJO [1] F. GERVILLA [4] C.J. GARRIDO [4]
A. RODRÍGUEZ-VEGA [2] R. LOZANO-SANTACRUZ [5] J.A. BLANCO-MORENO [2]

[1] **Departament de Cristal·lografia, Mineralogia i Dipòsits Minerals, Facultat de Geologia, Universitat de Barcelona**
Martí i Franquès, s/n, 08028, Barcelona, Spain. Proenza E-mail: japroenza@.ub.edu

[2] **Departamento de Geología, Instituto Superior Minero Metalúrgico de Moa**
Las Coloradas s/n, 83320, Moa, Holguín, Cuba.

[3] **Centro de Geociencias, Universidad Nacional Autónoma de México**
Campus Juriquilla, C.P. 76230 Juriquilla, Querétaro, México, and
Department of Geological Sciences, University of Colorado at Boulder
Boulder, Colorado 80309, USA.

[4] **Departamento de Mineralogía y Petrología, Facultad de Ciencias, Universidad de Granada**
Avenida Fuentenueva, s/n, 18002, Granada, Spain.

[5] **Instituto de Geología, Universidad Nacional Autónoma de México**
Coyoacán 04510, México, D.F., México.

ABSTRACT

The Téneme Formation is located in the Mayarí-Cristal ophiolitic massif and represents one of the three Cretaceous volcanic Formations established in northeastern Cuba. Téneme volcanics are cut by small bodies of 89.70 ± 0.50 Ma quarz-diorite rocks (Río Grande intrusive), and are overthrusted by serpentinized ultramafics. Téneme volcanic rocks are mainly basalts, basaltic andesites, andesites, and minor dacites, and their geochemical signature varies between low-Ti island arc tholeiites (IAT) with boninitic affinity (TiO_2 < 0.4 %; high field strength elements << N-type MORB) and typical oceanic arc tholeiites (TiO_2 = 0.5-0.8 %). Basaltic rocks exhibit low light REE/Yb ratios (La/Yb < 5), typical of intraoceanic arcs and are comparable to Maimón Formation in Dominican Republic (IAT, pre Albian) and Puerto Rican lavas of volcanic phase I (island arc tholeiites, Aptian to Early Albian). The mantle wedge signature of the Téneme Formation indicates a highly depleted MORB-type mantle source, without any contribution of E-MORB or OIB components. Our results suggest that Téneme volcanism represents a primitive oceanic island arc environment. If the Late Cretaceous age (Turonian or early Coniacian) proposed for Téneme Formation is correct, our results indicate that the Cretaceous volcanic rocks of eastern Cuba and the Dominican Republic are not segments of a single arc system, and that in Late Cretaceous (Albian-Campanian) Caribbean island arc development is not represented only by calc-alkaline (CA) volcanic rocks as has been suggested in previous works.

KEYWORDS | **Geochemistry. Volcanic rocks. Primitive-island arc. Téneme Formation. Cuba.**

INTRODUCTION

Donnelly and Rogers (1980) and Donnelly et al. (1990) distinguished three igneous series in the development of the circum-Caribbean Island Arc. The first stage of arc development is characterized by mid-ocean ridge basalts (MORB). The second stage is represented by the so-called "primitive island-arc" (PIA) (pre-Albian), similar in composition and tectonic setting to island-arc tholeiites (IAT); this volcanic activity appears to be contemporaneous with the MORB series. The third stage of Caribbean island arc development is represented by Late Cretaceous (Albian-Campanian) to Early Oligocene calc-alkaline (CA) volcanic rocks. In addition, Kerr et al. (1999) suggested that the oldest arc volcanism in the northern Caribbean region is a short-live boninitic arc, which predates the PIA series.

The PIA volcanic rocks consist of basalts, basaltic andesites and less common dacites and/or rhyolites. All these rocks are strongly altered by seawater. This process modified the mafic rocks to spilite, and the felsic rocks to keratophyre and quartz keratophyre. PIA volcanics in Greater Antilles include the following units from east to west (Fig. 1): Water Islands Formation in the Virgin Islands; pre-Robles Formation of eastern Puerto Rico; Los Ranchos and Tortue-Amina-Maimón Formations in Hispaniola; clasts of PIA rocks in pre-Camujiro sedimentary rocks near the province of Camagüey, and Los Pasos Formation in Central Cuba (Donnelly and Rogers, 1980; Donnelly et al., 1990; Lebron and Perfit, 1993, 1994; Iturralde-Vinent, 1994, 1996b, 1996c; Lewis et al., 1995, 2000, 2002; Díaz de Villalvilla, 1997; Díaz de Villalvilla et al., 1994; Simon et al., 1999; Lidiak and Jolly, 2002; Blein et al., 2003).

In addition, Lebron and Perfit (1994) suggested that the Téneme Fm in eastern Cuba could also belong to the PIA volcanism (Pre-Albian), because of the presence of tholeiite rocks as reported by Torrez and Fonseca (1990). However, up to the present work, no detailed petrochemical studies have been carried out to characterize the Téneme volcanic arc magma source, and its inclusion in the PIA series is uncertain.

In this paper, we provide new data on petrographic characteristics, mineral chemistry, and whole rock contents in major and trace elements (high field strength elements: HFSE and rare earth elements: REE) of the Téneme volcanic rocks of eastern Cuba. According to our data, we suggest that Téneme volcanism represents a primitive oceanic island arc environment, and that Cretaceous volcanic rocks of eastern Cuba and the Dominican Republic are not segments of a single arc system.

CRETACEOUS ARC-RELATED VOLCANIC ROCKS IN NORTHEASTERN CUBA

The geology of the northern part of eastern Cuba is characterized by the presence of the "Mayarí-Baracoa ophiolitic belt" (MBOB; Iturralde-Vinent, 1996a; Proenza et al., 1999a; Cobiella-Reguera, 2005), which includes two allochthonous massifs: the Mayarí-Cristal massif to the west and the Moa-Baracoa massif to the east (Fig. 2). The MBOB is a strongly faulted pseudotabular body that is ca. 170 km long, 10 to 30 km wide, and on average 3.5 km thick, and mainly comprised of harzburgite tectonites (Proenza et al., 1999a, b; Marchesi et al., 2003, in press). These ophiolitic rocks are in systematic tectonic contact with Cretaceous volcanic rocks.

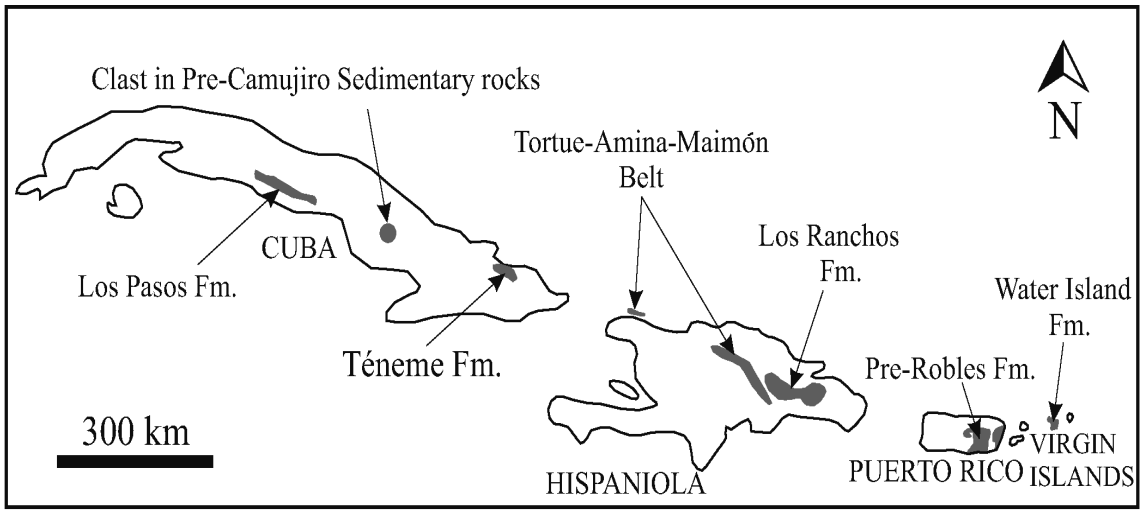

FIGURE 1 | **Distribution of the primitive island arc (PIA) series (gray shade) in Greater Antilles, based on the compilation of Simons et al. (1999).**

In northeastern Cuba three units of Cretaceous volcanic and sedimentary rocks have been distinguished, namely the Quibiján, Santo Domingo, and Téneme Formations (Knipper and Cabrera, 1974; Quintas, 1988, 1989; Quintas et al., 1994; Torres and Fonseca, 1990; Gyarmati and Leyé O'Conor, 1990; Gyarmati et al., 1997; Iturralde-Vinent, 1976, 1996a, 1996b; Kerr et., 1999; Iturralde-Vinent et al., this volume) (Fig. 2). Quibiján Fm crops out in the Moa-Baracoa massif, and has its type section along the Quibiján river basin (Quintas, 1988, 1989). According to Quintas (1988), the volcanic sequence is more than 500 m thick, and mainly consists of porphyritic and amygdaloidal basalts and tuffaceous rocks. In addition, several outcrops of Cretaceous volcanic rocks, which occur in tectonic contact with the serpentinized peridotites of the Moa-Baracoa massif, along the Moa-Baracoa road, have been reported as part of the Quibiján Fm (e.g. Morel and Duaba areas; Fig. 3A). At Morel these volcanic rocks consist of a sequence of pillowed basalts interbedded with cherts and hyaloclastites. Two samples analyzed by Kerr et al. (1999) exhibit island arc tholeiite affinity and were interpreted as formed in a back-arc basin.

At the type section south of the town of Calabazas, the Santo Domingo Fm is represented by tuffs and tuffaceous rocks intercalated with scarce limestone beds. Sills of porphyritic andesites also occur. The volcanic sequence is more than 2000 m thick (Iturralde-Vinent, 1976, 1996b). Iturralde-Vinent et al. (this volume), suggest that the Santo Domingo Fm is Turonian(?)-Campanian in age. No detailed geochemical studies have been performed to characterize the Santo Domingo volcanics, although Gyarmati et al. (1997) suggested a tholeiite and calc-alkaline affinity based on major element geochemistry.

Geochemical data from relatively immobile trace elements, including HFSE and REE, in the Quibiján (as defined by Quintas, 1988) and Santo Domingo Fms are not available. Thus, the geochemical affinity, magma source and tectonic setting of Quibiján and Santo Domingo volcanism are uncertain.

The Téneme Formation

Téneme Formation is located in the Mayarí-Cristal massif, west of the Sagua de Tánamo region (Fig. 2). According to the 1:500,000 Geological Map of Cuba (Linares et al., 1985), these volcanic rocks were included within the Santo Domingo Fm. Later, Téneme volcanics were formalized as an independent lithostratigraphic unit

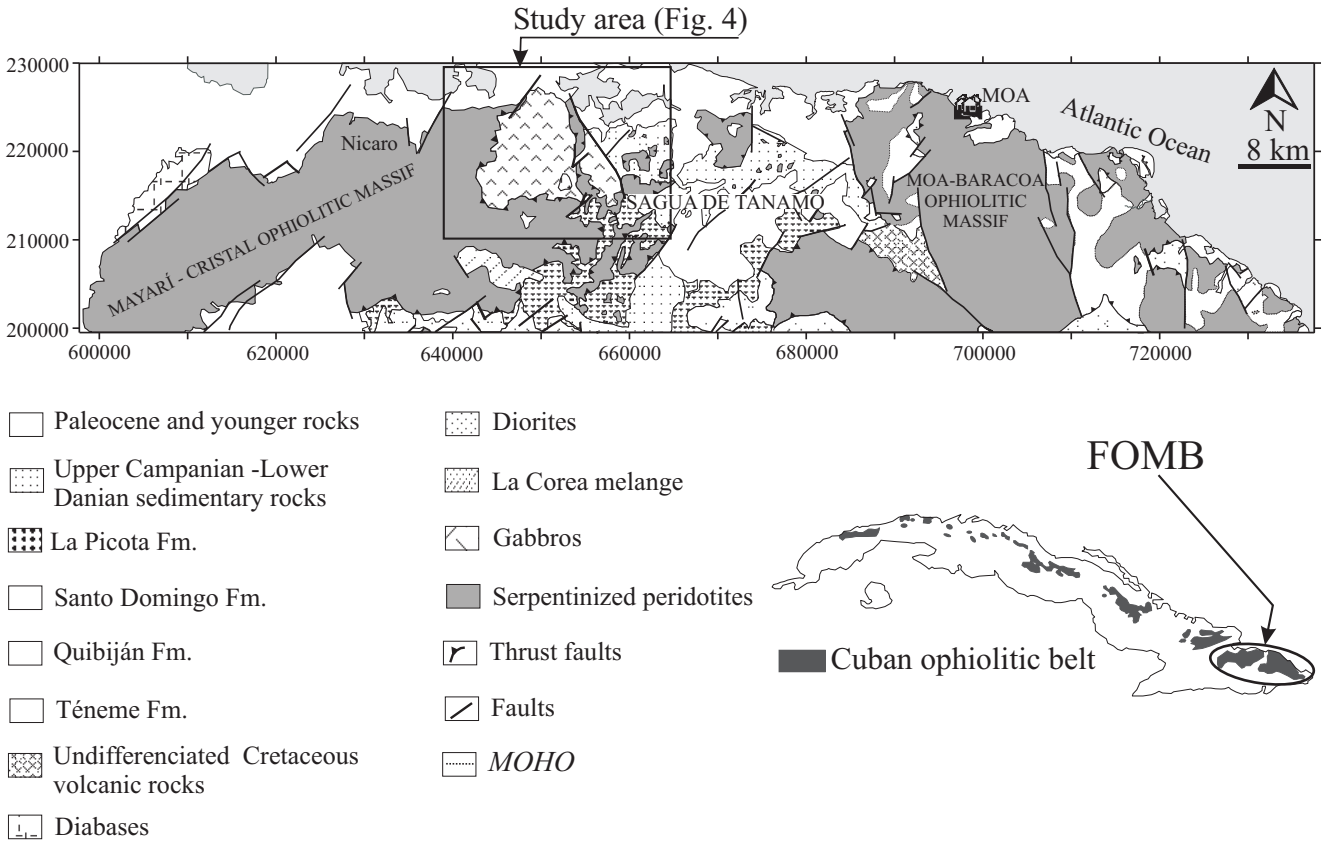

FIGURE 2 | **Geological map of the easternmost part of Cuba, showing the main outcrops of Cretaceous arc-related volcanic rocks.**

(Téneme Formation, see Geological Map 1:250,000 of the Republic of Cuba; Pushcharovsky et al., 1988). According to Iturralde-Vinent et al. (this volume), the age of Téneme Fm is Late Cretaceous. The fossil assemblage includes radiolaria and planktonic foraminifera that can be dated as Turonian to early Coniacian (*Marginotruncana*, *Whiteinella* spp.).

In the study region (Fig. 2), the Téneme Fm is exposed within an area of approximately 40 km^2 (Fig. 4), and is overthrusted by the ultramafic rocks of the Mayarí-Cristal ophiolitic massif (Fig. 3B). North of the study area, Téneme volcanics are unconformably overlayed by Paleogene volcanic sedimentary rocks of the Sabaneta Formation (Fig. 4), whereas toward the east they are in tectonic contact with Late Cretaceous-Paleocene sedimentary rocks (Micara and Picota Fms; Iturralde-Vinent, 1976; Quintas, 1989; Iturralde-Vinent et al., this volume).

The Téneme volcanic sequence has been studied in detail along the Río Grande (Adamovich et al., 1963; Knipper and Cabrera, 1974). These authors subdivided the volcanic sequence into three sections. The lower section is represented mainly by basaltic andesites, and reaches up to 500 m in thickness. The intermediate section is made up of basalts, basaltic andesites and spilites, and it is up to 1200 m thick. The upper section consists of a 300 m thick sequence of lavas, interbedded tuffs, and tuffaceous sandstones. Adamovich et al. (1963) and Knipper and Cabrera (1974) stated that Téneme Formation reaches up to 2000 m in thickness, but our field observations indicate this datum is overestimated. We consider that the thickness of the volcanic sequence is less than 1000 m.

Three small bodies of intrusive rocks are exposed toward the southeastern boundary of the study area. These plutonic rocks (Río Grande intrusive, Fig. 4) are medium to fine-grained, quartz diorites that exhibit a strong foliation defined by amphibole orientation.

SAMPLING AND ANALYTICAL PROCEDURES

Téneme volcanic rocks were sampled in their type section. A total of 24 samples were collected: 20 volcanics and 4 plutonic rocks from the intrusive outcrop in the southeast part of the study area (Fig. 4). In addition, two samples (M-1 and D-1) of the Quibiján Fm, from along the Moa-Baracoa road, were also analyzed for comparison. The sample M-1 was taken from the locality of Morel, the same area of samples QUI1 and QUI2 of Kerr et al. (1999), and sample D-1 was collected in the locality of Duaba, very near of Baracoa city.

Chemical analyses of the mineral phases were carried out with a CAMECA SX 50 electron microprobe at the University of Barcelona as described by Proenza et al. (1999a).

Major elements and selected trace elements (Y, Zr, V, Cr, Co, Ni, Cu and Zn) contents were determinated by XRF at the *Universidad Nacional Autónoma de México (UNAM)*. Li, Cs, Be, Sc, Zn, Ga, Nb, Ta, Mo, Sn, Tl, Pb, U, Th and REE were measured by ICP-MS at the *Centro de Instrumentación Científica*, at the University of Granada.

Hornblende mineral separates from quartz diorite samples Tm-35 (36.5 mg) and Tm-37 (110.0 mg) were produced and later irradiated for 8 hours in package KD33 at the TRIGA reactor at the U.S. Geological Survey in Denver. The monitor mineral used was Fish Canyon Tuff sanidine (FCT-3) with an age of 27.79 Ma (Kunk et al., 1985; Cebula et al., 1986). Both hornblende separates were analyzed at the U.S. Geological Survey Argon Thermochronology lab in Denver on a VG Isotopes Ltd., Model 1200 B Mass Spectrometer fitted with an electron multiplier using the $^{40}Ar/^{39}Ar$ step-heating method of dating. For additional information on both, analytical procedures and data reduction, see Kunk et al. (2001). We used the

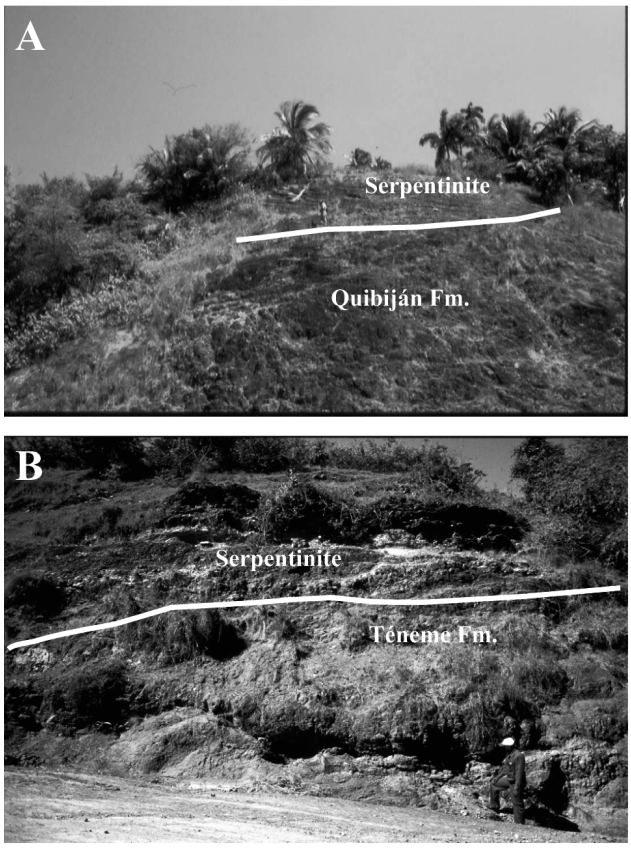

FIGURE 3 | **Outcrop pictures of the Quibiján (A) and Téneme (B) Fms at the Moa-Baracoa and the Mayorí-Cristal massives, respectively. These volcanic rocks are overthrusted by ultramafic rocks (mainly serpentinite and serpentinized harzburgite) of the Mayarí-Baracoa ophiolitic belt. See Fig. 1 for location.**

decay constants recommended by Steiger and Jager (1977). Plateau ages, not present, are identified when three or more contiguous steps in the age spectrum agree in age, within the limits of analytical precision, and contain more than 50% of the $^{39}Ar_K$ released from the sample. Average ages are calculated in the same manner as plateau ages except that contiguous steps do not agree in age.

PETROGRAPHIC DESCRIPTION AND MINERAL CHEMISTRY OF THE TÉNEME VOLCANICS

Volcanic rocks of the Téneme Fm are mainly composed of basalts, basaltic andesites, andesites, and minor dacites. In general, Téneme volcanics underwent extensive hydrothermal processes that led to formation of abundant quartz veins.

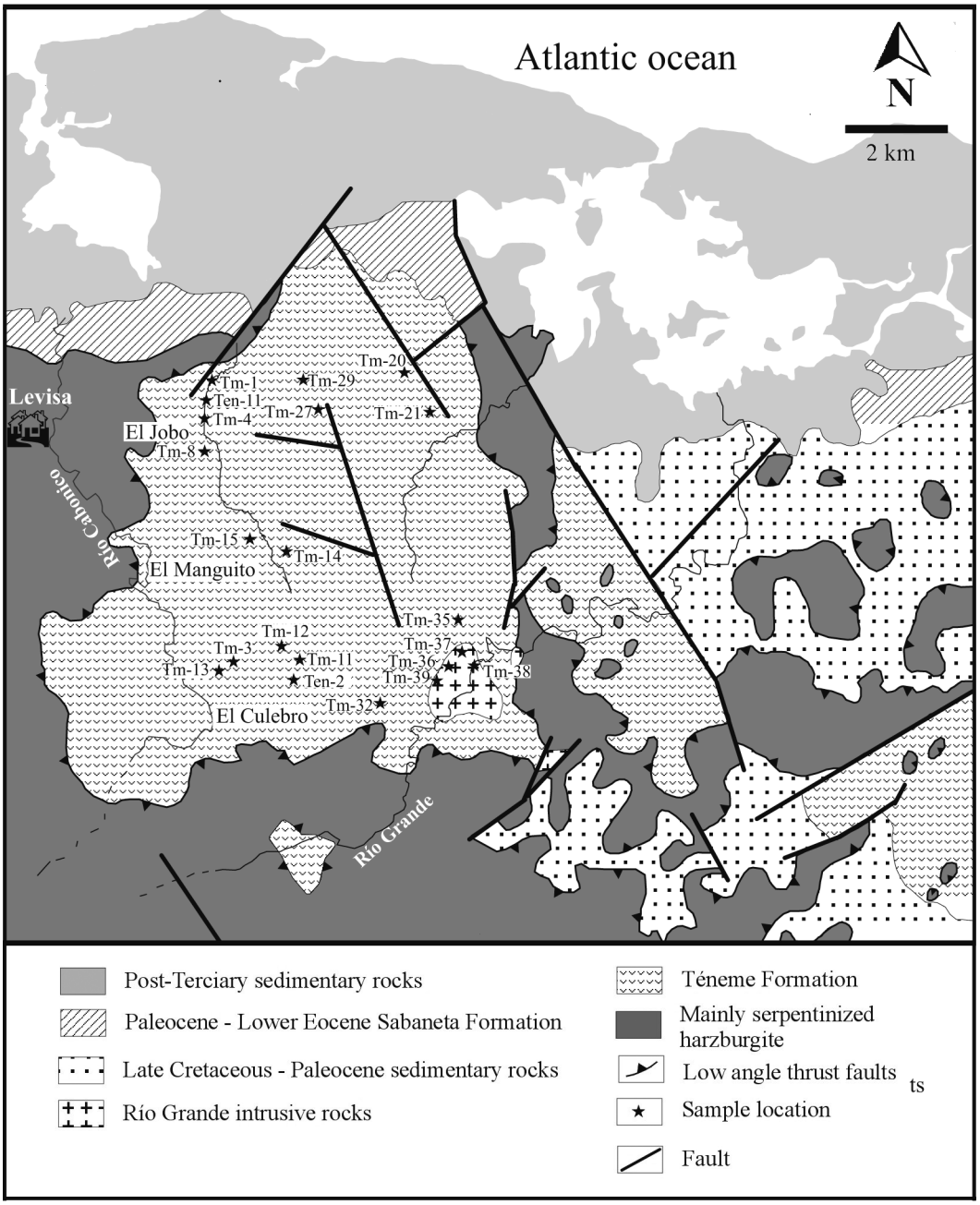

FIGURE 4 | **Geological map of the area of Téneme volcanics. Geology based on the compilation map of Gyarmati and Leyé O'Conor (1990). Sample locations are indicated.**

In thin section the volcanic rocks mainly show a porphyritic texture, but glomeroporphyritic and aphyric textures are also observed. The samples contain relict phenocrysts or microphenocrysts of clinopyroxene, plagioclase, Cr-spinel, and altered (serpentinized and/or chloritized) olivine and orthopyroxene. Primary amphibole is absent in all studied samples. The groundmass comprises plagioclase and clinopyroxene microlites, and devitrified glass. Accessory minerals include apatite and subhedral magnetite. Alteration products are chlorite, albite, epidote, clinozoisite, calcite and quartz. All samples exhibit zeolite and prehnite-pumpellyite facies metamorphism or lower greenschist grade that overprinted the primary groundmas.

Clinopyroxene

Representative analyses of clinopyroxenes from Téneme volcanic rocks are displayed in Table 1. Clinopyroxene analyses are plotted in the enstatite-diopside-hedenbergite-ferrosilite quadrilateral, following the classification of Morimoto et al. (1989). They lie in the augite field and predominantly in the Mg-rich portion (Fig. 5A). Clinopyroxene phenocrysts from basaltic rocks have low Ti contents (Table 1), and plot in the island arc tholeiite (Fig. 5B) field of Leterrier et al. (1982). In addition, the composition of Téneme clinopyroxene crystals is similar to that observed in suprasubduction zone (SSZ) ophiolites

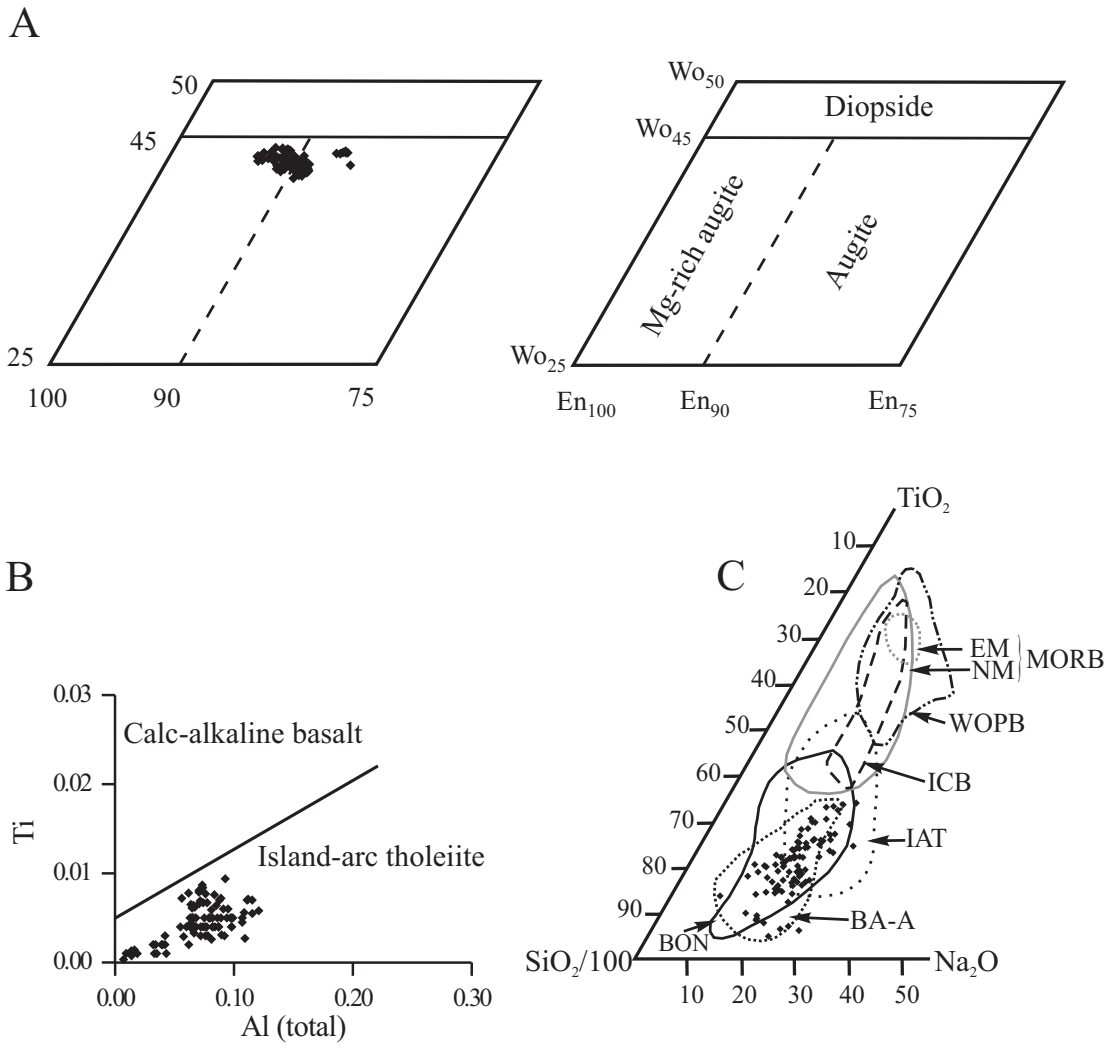

FIGURE 5 | **A) Compositions of clinopyroxene phenocrysts of basaltic rocks from the Téneme Fm, expressed in terms of wollastonite-enstatite-ferrosilite abundances. Pyroxene nomenclature is from Morimoto et al. (1989). B) Variation of Ti versus total Al in clinopyroxene phenocrysts from basaltic rocks of the Téneme Fm. Notice as all samples plot into the island arc tholeiite field of Leterrier et al. (1982). C) TiO_2-Na_2O-SiO_2/100 discrimination diagram (Beccaluva et al., 1989) for clinopyroxene from basaltic rocks of the Téneme Fm. NM: normal MORB; EM: enriched MORB; ICB: Iceland basalts; IAT: island arc tholeiites; BON: boninites; BA-A: intraoceanic fore arc basalts and andesites.**

TABLE 1 **Representative analyses of clinopyroxenes from Téneme volcanics.**

	1	2	3	4	5	6	7	8	9	10	11	12
SiO_2	53.63	53.27	52.00	52.08	53.97	54.08	52.62	52.83	52.83	52.28	53.05	52.99
TiO_2	0.11	0.12	0.28	0.24	0.04	0.06	0.14	0.16	0.19	0.17	0.19	0.16
Al_2O_3	1.34	1.54	1.60	1.68	0.99	0.94	2.02	1.90	2.07	2.26	1.50	1.71
Fe_2O_3	0.79	1.64	1.81	1.47	1.29	1.65	2.36	1.53	1.85	2.33	1.30	1.93
MgO	18.74	18.65	14.51	14.38	18.77	19.65	18.00	17.72	17.61	17.54	17.77	17.75
CaO	20.45	21.21	20.70	21.02	21.26	21.06	20.38	20.74	20.69	20.58	19.40	19.41
MnO	0.20	0.13	0.36	0.13	0.16	0.13	0.17	0.17	0.11	0.15	0.22	0.21
FeO	3.85	2.48	8.47	8.62	2.91	1.88	3.71	4.09	4.66	4.17	6.17	6.00
Na_2O	0.12	0.17	0.25	0.26	0.17	0.14	0.21	0.20	0.15	0.15	0.14	0.17
K_2O	0.00	0.00	0.02	0.01	0.00	0.02	0.01	0.00	0.00	0.00	0.01	0.00
Total	99.22	99.21	99.99	99.87	99.56	99.60	99.60	99.33	100.16	99.64	99.74	100.33
Si	1.96	1.95	1.94	1.95	1.97	1.96	1.93	1.94	1.93	1.92	1.95	1.94
Ti	0.00	0.00	0.01	0.01	0.00	0.00	0.00	0.00	0.01	0.01	0.01	0.00
Al	0.06	0.07	0.07	0.07	0.04	0.04	0.09	0.08	0.09	0.10	0.07	0.07
Fe^{3+}	0.02	0.05	0.05	0.04	0.04	0.05	0.07	0.04	0.05	0.06	0.04	0.05
Mg	1.02	1.02	0.81	0.80	1.02	1.06	0.98	0.97	0.96	0.96	0.97	0.97
Ca	0.80	0.83	0.83	0.84	0.83	0.82	0.80	0.82	0.81	0.81	0.76	0.76
Mn	0.01	0.00	0.01	0.00	0.01	0.00	0.01	0.01	0.00	0.01	0.01	0.01
Fe^{2+}	0.12	0.08	0.26	0.27	0.09	0.06	0.11	0.13	0.14	0.13	0.19	0.18
Na	0.01	0.01	0.02	0.02	0.01	0.01	0.02	0.01	0.01	0.01	0.01	0.01
K	0.00	0.00	0.00	0.00	0.00	0.00	0.00	0.00	0.00	0.00	0.00	0.00

Cations calculated on the basis of 6 oxygens

and their modern analogues (e.g. Beccaluva et al., 1989; Bortolotti et al., 2002). On the SiO_2/100-TiO_2-Na_2O discrimination diagram, the clinopyroxene crystals from the Téneme volcanic rocks plot in the intraoceanic forearc basalts and basaltic andesite field (Fig. 5C).

Cr-spinel

The presence of Cr-spinel in Téneme basaltic rocks is in accordance with the high Cr content of the whole rock (up to 1027 ppm in sample Tm-29; Table 2). Cr-spinels have high Cr# ([Cr/(Cr+Al)] ≥0.8) and low TiO_2 contents (≤0.25 wt %) (Table 2). This composition is similar to that of Cr-spinel reported from Troodos volcanics, and comparable to that found in boninites (Fig. 6A). In general, Cr-spinels are depleted in Fe_2O_3, and can be interpreted as close to their magmatic compositions. The lowest values of Mg/(Mg+Fe^{2+}) probably result from partial re-equilibration of Cr-spinel crystals with the liquid during groundmass crystallization.

According to Barnes and Roeder (2001), there is a petrogenetic link between some ophiolite complexes and boninitic lavas. In this sense, accessory chromite in dunite from the easternmost part of the Mayarí-Cristal ophiolitic massif (Sagua de Tánamo region) have Cr# just above the field of abyssal peridotites, and similar to those in equilibrium with IAT and boninitic magmas (Fig 6B). Thus, some Sagua de Tánamo dunites probably formed when depleted IAT or boninite melts passed through mantle harzburgite. Such magmas could be represented by Cr-rich spinel-bearing Téneme volcanics.

GEOCHEMISTRY OF TÉNEME VOLCANIC ROCKS

Geochemical classification

Studies on element mobility during alteration processes show that the most mobile elements are K, Na, Rb, Ba, Sr, Ca, Mg, Si, Fe and Mn. In contrast, Ti, Al, Nb, Y, Th, Ta, Zr, Hf, as well as most of the REE (mainly MREE and HREE) are considered to be practically immobile. In order to examine the geochemical signature of the Téneme rocks immobile HFSE and REE have been preferentially considered.

Analyzed samples from the Téneme Fm are classified in two groups according to silica content: basaltic type (50 < SiO_2 < 60 wt%) and intermediate type (60 < SiO_2 <

70 wt% for samples Ten-3, Tm-12 and Tm-13). They show relatively high MgO contents (5-10 wt%, except for one sample) and exhibit a clear IAT affinity (TiO_2 = 0.28-0.83 wt%, Zr = 28-96 ppm, Y = 7-17 ppm; P_2O_5 < 0.1 wt%). Two analyzed samples from the Quibiján Formation (samples M-1 and D-1) are basaltic rocks with TiO_2 contents above 1 wt% (Table 3).

Hawkesworth et al. (1993a, 1993b), subdivided island arc basaltic rocks on the basis of their LREE/HREE ratio: (1) low-LREE series represent intraoceanic arcs, and (2) high-LREE series are representative of arcs developed in proximity to continental margins. On the La-Yb variation diagram (Fig. 7) Téneme and Quibiján basaltic rocks fall within the low-LREE/Yb island arc basalt field (La/Yb < 5), similar to those from the Maimón Formation in Dominican Republic (IAT, pre Albian; Lewis et al., 2002), and to the Puerto Rican lavas of volcanic phase I (IAT, Aptian to Early Albian; Jolly et al., 2001).

REE and spider diagrams of the Téneme volcanics

Téneme volcanic rocks exhibit slight REE enrichment, and MREE and HREE depletion with respect to N-type MORB (Fig. 8A). The relative enrichment in LREE may be linked to interaction with subduction-related fluids.

Similar LREE enrichment and MREE and HREE depletion with respect to N-type MORB characterize PIA meta-basaltic rocks of Cerro de Maimón (southern margin of the Maimón Fm, Dominican Republic; Lewis et al., 2000), as illustrated in Fig. 8B. This figure shows that there is a strong similarity among REE patterns of Téneme basaltic rocks and those of meta-basalts from the Maimón Formation, and of boninites from the western Pacific island arcs.

In contrast to Téneme volcanics, the Morel basalt (sample M-1) has a relatively flat REE pattern similar to N-MORB, confirming the results reported by Kerr et al. (1999). This REE pattern exhibits a slight peak at Nd-Sm, which is typical of BABB (Back-arc basin basalts) produced during the earliest stages of back-arc basin spreading (Hawkins and Allan, 1994; Meffre et al., 1996). However, the Duaba basalt (sample D-1) shows a slight enrichment in LREE, with a flat MREE to HREE segment (Fig. 8C).

As generally reported for island arc suites, MORB-normalized multielement plots reveal that Téneme basaltic rocks are enriched in LILE with respect to LREE and depleted in HFSE, MREE and HREE (Fig. 9A). These patterns are similar to those reported for metabasaltic rocks from the Maimón and Los Rancho Formations in Dominican Republic (Fig. 9B) (Lewis et al., 2000, 2002), interpreted as original basalts formed respectively in the forearc and in the axial region of a nascent primitive island arc (see Lewis et al., 2000, 2002). In contrast, MORB-normalized multielement patterns of Morel and Duaba basalts indicate a more fertile

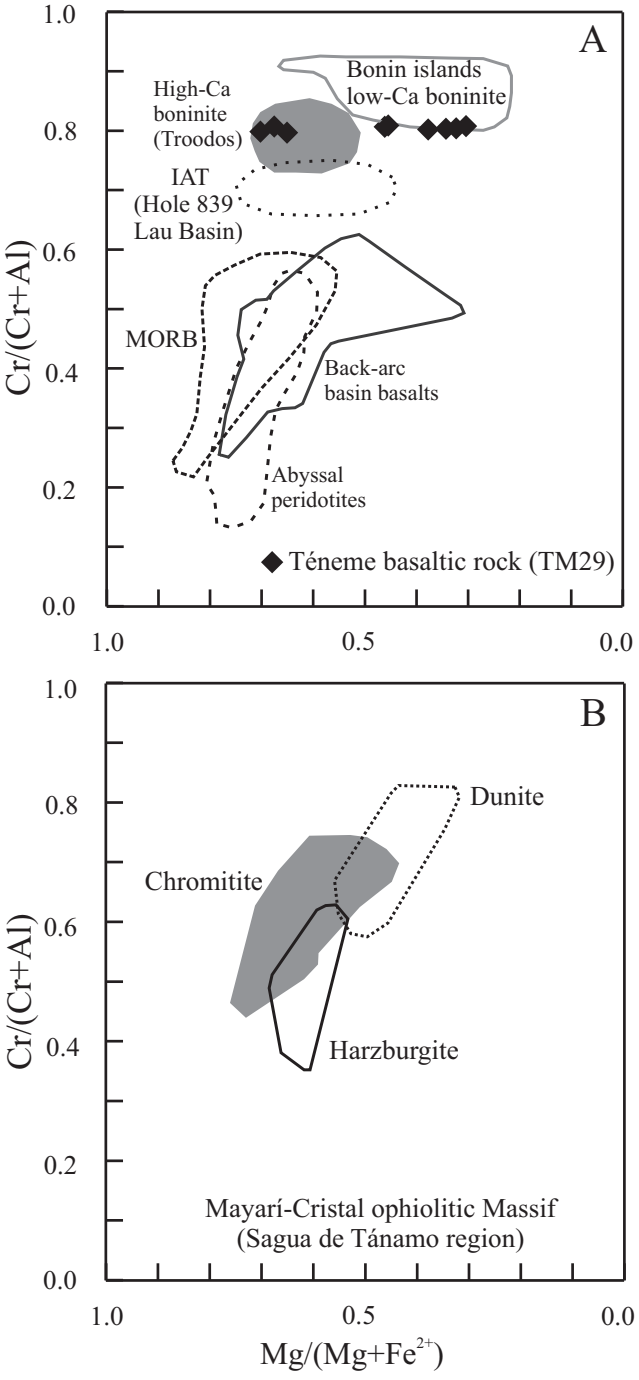

FIGURE 6 | **A) Compositions of chromite from Téneme volcanics (sample Tm-29) compared to chromite of various magma types. B) Summary of chromite data from the eastern part of Mayarí-Cristal ophiolitic massif (Sagua de Tánamo region; Proenza et al., 1999; 2003), which is in tectonic contact with the Téneme volcanics. Fields of different magma types and abyssal peridotites are from compilation of Metzger et al. (2002).**

TABLE 2 **Representative analyses of chromian spinels from Téneme volcanics.**

	1	2	3	4	5	6	7	8	9	10
TiO_2	0.21	0.21	0.23	0.25	0.19	0.15	0.19	0.20	0.20	0.17
Al_2O_3	9.20	9.89	9.92	9.84	9.21	9.11	9.49	9.39	9.42	9.03
V_2O_3	0.13	0.21	0.10	0.12	0.16	0.15	0.09	0.15	0.07	0.09
Cr_2O_3	55.28	58.04	58.76	58.69	55.34	54.74	56.81	56.24	56.22	55.33
Fe_2O_3	4.71	5.23	5.63	5.43	4.37	3.97	4.39	5.21	4.38	4.40
MgO	6.18	13.19	14.69	14.60	6.46	4.64	8.95	8.96	7.30	5.86
MnO	0.95	0.40	0.24	0.26	0.83	0.95	0.61	0.69	0.81	0.81
FeO	23.13	13.23	11.29	11.29	22.59	25.11	19.30	19.24	21.71	23.54
NiO	0.13	0.09	0.12	0.15	0.19	0.14	0.16	0.20	0.18	0.15
ZnO	0.52	0.03	0.05	0.02	0.67	0.80	0.18	0.27	0.26	0.45
Total	100.44	100.54	101.02	100.64	100.02	99.76	100.16	100.54	100.54	99.83
Ti	0.04	0.04	0.05	0.05	0.04	0.03	0.04	0.04	0.04	0.04
Al	2.95	3.01	2.98	2.97	2.96	2.98	2.99	2.95	2.99	2.92
V	0.03	0.04	0.02	0.02	0.04	0.03	0.02	0.03	0.02	0.02
Cr	11.91	11.85	11.83	11.86	11.95	12.01	12.00	11.85	11.98	12.02
Fe^{3+}	0.97	1.02	1.08	1.05	0.90	0.83	0.88	1.05	0.89	0.91
Mg	2.51	5.08	5.57	5.56	2.63	1.92	3.56	3.56	2.93	2.40
Mn	0.22	0.09	0.05	0.06	0.19	0.22	0.14	0.16	0.18	0.19
Fe^{2+}	5.27	2.86	2.40	2.41	5.16	5.83	4.31	4.29	4.89	5.41
Ni	0.03	0.02	0.02	0.03	0.04	0.03	0.03	0.04	0.04	0.03
Zn	0.10	0.01	0.01	0.00	0.14	0.16	0.04	0.05	0.05	0.09
Total	24.03	24.00	24.01	24.00	24.04	24.05	24.02	24.02	24.02	24.03

Cations calculated on the basis of 32 oxygens

source than for the Téneme basaltic rocks. However, Duaba sample has a more marked Nb anomaly than Morel basalt (Fig. 9C).

Magma source and tectonic setting

The Téneme basaltic rocks have IAT affinity, with a TiO_2 content ranging from 0.28 to 0.53 wt %. Only one sample (Tm-21) is relatively TiO_2-rich (0.83 wt %). In contrast, the Quibiján volcanics exhibit TiO_2 contents ranging from 1.04 (sample D-1) to 1.90 (M-1) wt % and plot in the field of basalts generated at mid-ocean ridge setting (Fig. 10A). On the Th-Hf/3-Nb/16 diagram (Fig. 10B) Téneme basaltic rocks and Duaba basalt (D-1) have a supra-subduction zone (SSZ) signature, whereas Morel sample (M-1) lies in the overlap zone of BABB and MORB fields.

In the Cr-Y diagram (Fig. 11A), all the Téneme basaltic rocks plot in both the IAT and boninite fields (mainly along the high-Ca boninites crystallization vector), whereas values exhibited by Quibiján samples are proper to the BABB and MORB fields. On the TiO_2-Zr diagram (Fig. 11B) the Téneme basaltic rocks plot within and close to the field of the Izu-Bonin-Mariana (IBM) forearc boninites, whereas the Quibiján volcanics follow

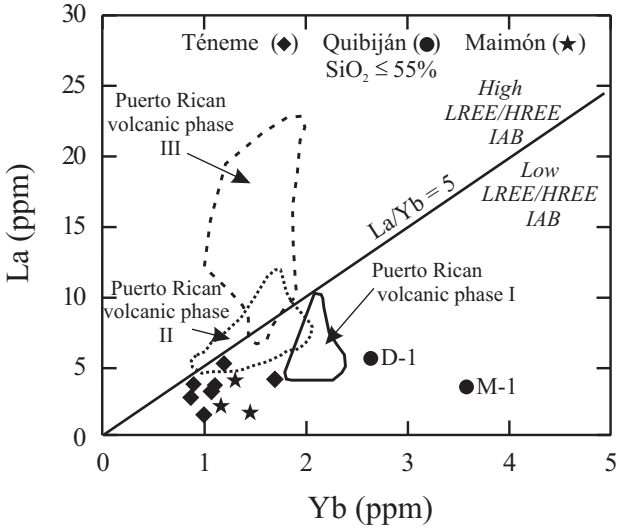

FIGURE 7 **La-Yb abundances in Téneme and Quibiján volcanic rocks. Fields of Central Puerto Rican volcanic phases are from Jolly et al. (2001), and data of Maimón Fm is taken from Lewis et al. (2000, 2002).**

TABLE 3 | **Representative major-elements (wt%) and trace elements (ppm) analyses from the Téneme volcanic rocks (Lt-1, Tm-21, Tm-29, Tm-14, Tm-1, Ten-1, Tm-20, Ten-2, Tm-8), Río Grande intrusive rocks (Tm-35, Tm-37, Tm-38) and Quibiján basalts (M-1 and D-1).**

	Lt-1	Tm-21	Tm-29	Tm-14	Tm-1	Ten-1	Tm-20	Ten-2	Tm-8	Tm-35	Tm-37	Tm-38	Tm-39	M-1	D-1
SiO_2	50.21	50.51	52.44	54.53	55.95	55.45	58.19	57.63	59.75	59.66	59.19	58.01	58.80	47.35	46.23
TiO_2	0.51	0.83	0.53	0.37	0.28	0.46	0.45	0.40	0.39	0.41	0.44	0.47	0.47	1.77	1.04
Al_2O_3	15.80	17.68	11.81	14.23	12.77	18.86	14.55	15.73	15.39	17.97	18.47	18.08	18.09	14.01	14.08
FeO*	9.19	10.44	8.64	8.00	7.43	7.03	7.46	6.85	6.60	6.39	6.26	7.15	7.18	11.25	13.40
MnO	0.12	0.19	0.12	0.13	0.13	0.11	0.12	0.11	0.08	0.13	0.13	0.15	0.15	0.19	0.25
MgO	10.44	4.88	9.95	8.00	9.17	4.27	5.59	5.15	7.73	2.34	2.39	2.78	2.65	7.20	8.77
CaO	8.53	8.04	11.38	9.24	8.32	7.84	10.06	9.05	0.49	7.53	7.57	7.63	7.85	12.25	8.21
Na_2O	1.47	3.29	2.22	1.42	2.69	2.79	1.51	1.69	4.49	2.85	2.92	2.88	2.31	1.71	2.91
K_2O	0.32	0.85	1.42	0.71	0.28	0.50	0.22	0.25	0.22	0.61	0.63	0.46	0.37	0.50	0.03
P_2O_5	0.04	0.10	0.08	0.05	0.03	0.08	0.06	0.06	0.07	0.07	0.08	0.08	0.09	0.16	0.20
LOI	4.11	3.40	1.25	3.78	3.09	3.08	2.26	3.55	4.82	2.47	2.34	2.85	2.69	4.06	5.33
Total	100.76	100.18	99.86	100.48	100.15	100.47	100.48	100.47	100.03	100.43	100.42	100.54	100.65	100.45	100.44
Y	9.00	13.00	17.00	6.00	9.00	11.00	10.00	10.00	7.00	13.00	13.00	15.00	13.00	33.00	21.00
Zr	75.00	51.00	61.00	52.00	28.00	96.00	60.00	60.00	83.00	53.00	42.00	56.00	50.00	119.00	103.00
V	245.00	325.00	199.00	187.00	185.00	190.00	199.00	170.00	218.00	161.00	165.00	178.00	156.00	359.00	345.00
Cr	239.00	51.00	1027.00	293.00	500.00	45.00	194.00	171.00	94.00	50.00	54.00	60.00	21.00	161.00	596.00
Li	18.32	9.26	1.46	12.99	7.15	8.56	8.23	10.66	17.33	5.62	5.75	7.56	6.41	9.94	25.38
Rb	3.78	8.44	28.76	8.27	3.21	5.35	3.05	4.29	2.43	13.25	13.16	9.47	7.80	5.11	0.06
Cs	0.30	0.22	0.15	0.21	0.17	0.30	0.05	0.09	0.19	0.39	0.67	0.49	0.47	0.15	0.14
Be	0.57	0.41	0.44	0.32	0.36	0.51	0.51	0.64	0.40	0.49	0.28	0.17	0.23	0.61	0.57
Sr	276.02	323.54	125.46	358.00	291.88	581.81	236.74	333.35	68.10	134.80	146.64	138.83	118.50	58.18	78.06
Ba	307.23	421.20	563.50	135.27	116.44	627.09	89.41	232.74	81.32	299.58	449.64	289.67	191.31	8.02	36.91
Sc	34.85	38.28	31.10	35.96	33.15	30.04	31.80	30.82	29.62	21.94	20.69	25.65	25.22	45.01	35.33
Co	41.09	36.73	62.39	39.02	45.23	71.32	57.47	51.58	30.26	44.13	43.41	41.73	42.73	44.94	47.11
Ni	94.77	33.23	587.65	66.09	122.25	87.26	64.82	761.25	52.05	37.75	122.82	98.17	24.81	65.21	347.72
Cu	77.70	144.04	21.60	78.52	54.39	72.62	54.32	35.84	141.86	8.45	10.47	10.83	4.86	53.41	55.83
Zn	62.07	96.57	60.40	63.95	55.92	57.87	53.43	59.30	156.55	45.68	43.32	51.24	46.98	97.61	113.10
Ga	18.05	18.35	10.16	14.38	11.59	19.22	17.18	16.31	16.86	18.28	18.62	18.37	18.57	20.96	16.40
Nb	1.05	1.31	1.05	1.35	1.16	1.19	0.68	0.96	0.61	1.39	1.43	1.61	1.54	3.00	1.69
Ta	0.18	0.35	0.24	0.39	0.42	0.30	1.43	0.30	0.17	0.74	0.72	0.63	0.67	0.39	0.32
Hf	1.66	3.35	1.17	3.36	3.14	1.83	1.04	1.39	1.24	0.38	0.36	0.43	0.26	2.99	4.00
Mo	3.93	3.22	46.50	2.30	1.89	13.91	1.73	158.89	5.37	6.52	24.11	20.02	3.46	1.50	3.62
Sn	0.08	0.19	0.52	0.23	0.04	0.11	0.39	0.27	0.00	0.42	0.35	0.33	0.11	0.27	0.58
Tl	0.06	0.08	0.24	0.06	0.02	0.09	0.02	0.01	0.01	0.08	0.09	0.06	0.05	0.02	0.01
Pb	2.82	2.41	0.91	1.88	1.90	3.61	4.51	2.77	2.47	1.29	1.37	1.28	0.88	0.38	2.41
U	0.69	0.38	0.25	0.32	0.38	0.65	0.35	0.53	0.42	0.68	0.26	0.32	0.23	0.27	0.33
Th	0.68	0.58	0.32	0.61	0.46	0.87	0.39	0.66	0.62	0.51	0.76	0.86	0.77	0.17	0.70
La	3.80	4.11	3.74	3.00	1.60	7.60	3.67	5.41	9.35	5.17	5.34	5.42	4.66	3.68	5.69
Ce	9.25	11.65	9.94	8.69	4.75	17.44	9.19	11.87	18.99	10.75	11.24	11.88	9.92	11.87	15.63
Pr	1.26	1.73	1.55	1.17	0.65	2.33	1.36	1.65	2.64	1.39	1.46	1.55	1.35	2.06	2.53
Nd	5.96	8.48	7.53	5.10	2.81	9.71	6.68	7.22	11.29	6.28	6.02	7.26	6.14	11.33	12.50
Sm	1.37	2.51	2.19	1.43	0.95	2.33	1.93	1.71	2.48	1.56	1.55	1.90	1.72	4.07	3.54
Eu	0.63	0.91	0.86	0.51	0.39	0.98	0.62	0.61	0.87	0.74	0.85	0.75	0.69	1.37	1.16
Gd	1.35	2.92	2.09	1.56	1.35	2.38	1.75	1.65	2.48	1.73	1.63	2.04	1.79	5.26	3.83
Tb	0.21	0.50	0.34	0.24	0.23	0.38	0.29	0.29	0.38	0.29	0.28	0.35	0.30	0.91	0.65
Dy	1.33	2.98	2.10	1.48	1.45	2.41	1.84	1.95	2.45	2.05	1.94	2.37	2.07	6.21	4.18
Ho	0.29	0.64	0.43	0.30	0.33	0.53	0.41	0.41	0.51	0.46	0.43	0.56	0.50	1.37	0.93
Er	0.85	1.76	1.20	0.86	0.95	1.49	1.19	1.23	1.41	1.39	1.23	1.56	1.45	3.81	2.60
Tm	0.13	0.27	0.18	0.13	0.15	0.24	0.19	0.18	0.22	0.23	0.20	0.24	0.22	0.57	0.41
Yb	0.90	1.71	1.10	0.88	1.01	1.51	1.07	1.19	1.43	1.43	1.34	1.51	1.46	3.58	2.64
Lu	0.14	0.26	0.16	0.14	0.16	0.25	0.16	0.18	0.20	0.23	0.23	0.24	0.23	0.49	0.40

the MORB trend. The increase in TiO_2 with a slight increase in Zr is typical of the tholeiitic suite, whereas IBM arc boninitic rocks exhibit a trend characterized by increasing Zr at low concentration of TiO_2. Hence, the Téneme volcanic rocks show the characteristic Zr enrichment of many Tertiary boninite suites. Téneme and Quibiján volcanics also differ in terms of LREE/MREE, as illustrated in La/Sm versus TiO_2 diagrams (Fig. 11C). Téneme rocks mainly plot in the field of IBM and North Tonga boninites, whereas the Morel sample plots within to the field of Lau back-arc basin, and the Duaba sample close to Mariana arc rocks.

In addition, the plot of Zr/Yb vs Nb/Yb (Fig. 12A) reflects that both Téneme and Quibiján volcanic rocks from eastern Cuba consistently exhibit geochemical con-

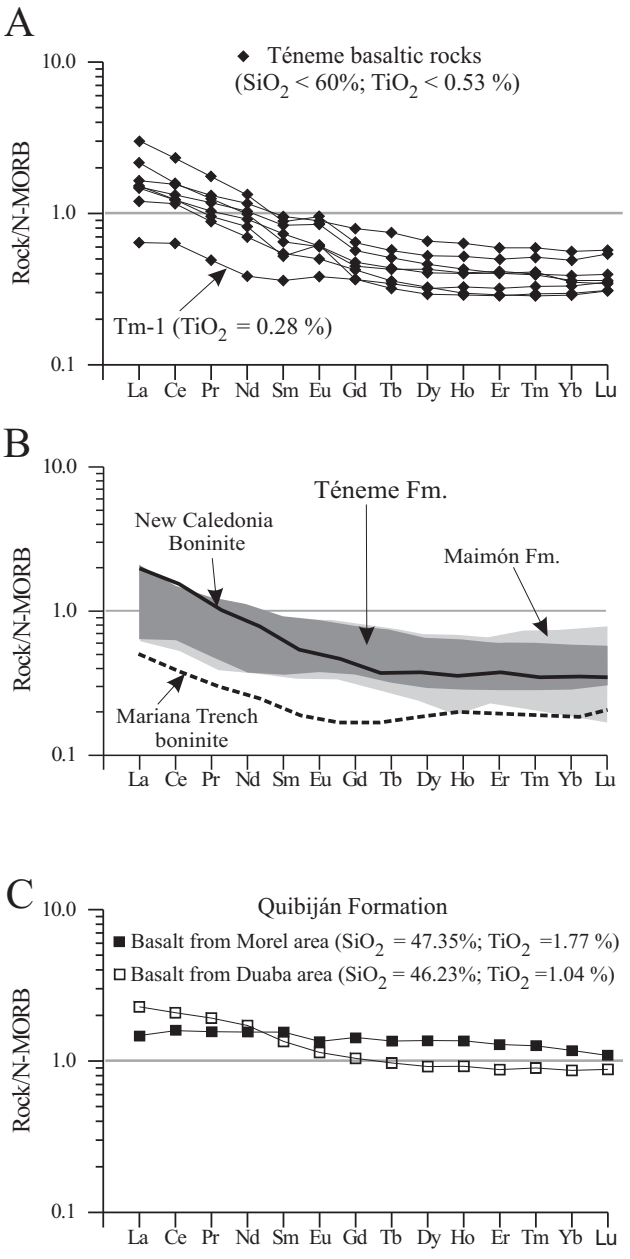

FIGURE 8 **A) N-MORB normalized REE patterns (Sun and McDonough, 1989) for the Téneme volcanic rocks. B) Comparison of N-MORB normalized REE patterns (Sun and McDonough, 1989) for Téneme basaltic rocks with: 1) metabasalts and mafic schists of the Maimón Fm (Lewis et al., 2002), and 2) western Pacific boninites (Pearce et al., 1992). C) N-MORB normalized REE patterns (Sun and McDonough, 1989) for the Quibiján basalts (Morel and Duaba areas).**

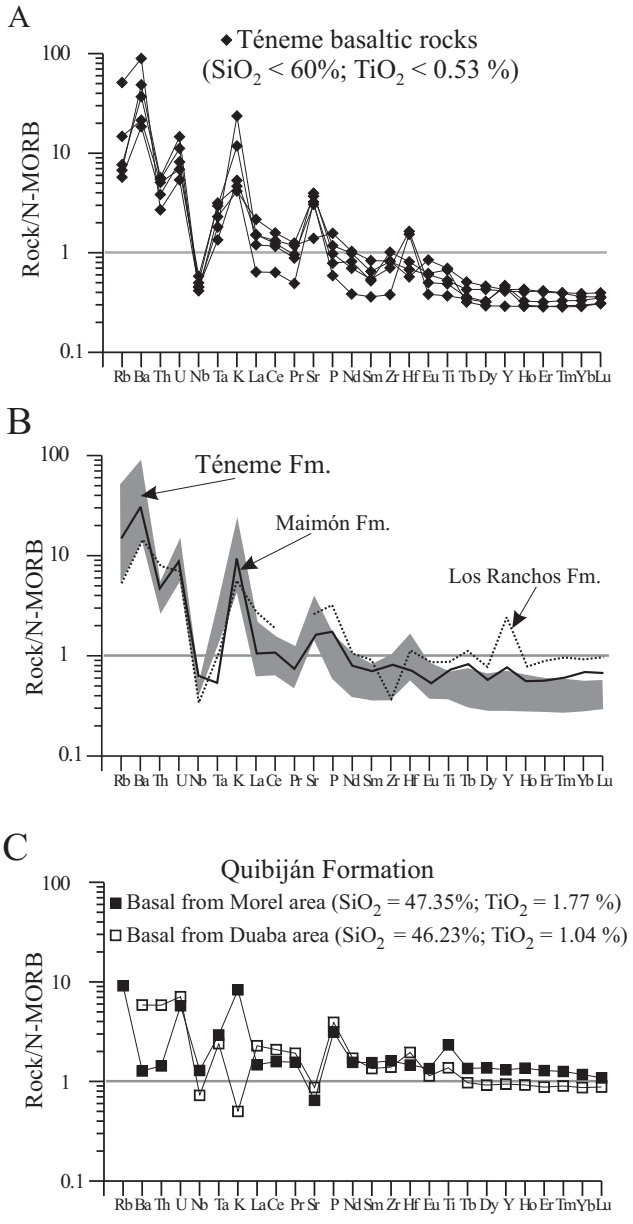

FIGURE 9 **A) N-MORB normalized multielemental diagrams (Sun and McDonough, 1989) for the Téneme volcanic rocks. B) Comparison of N-MORB normalized multielemental diagrams (Sun and McDonough, 1989) for the Téneme basaltic rocks with representative metabasalts and mafic schists of the Maimón and Los Ranchos Fms. Average geochemical analyses for Maimón and Los Ranchos Fms are taken from Lewis et al. (2002). C) N-MORB normalized multielemental diagrams (Sun and McDonough, 1989) for the Quibiján basalts (Morel and Duaba areas).**

tributions from relative depleted mantle sources. These results suggest that the basement beneath eastern Cuba in Upper Cretaceous was a depleted or normal N-MORB-type mantle. Téneme basaltic rocks and the sample of Duaba (D-1) have high Th contents associated with derivation from arc mantle sources (Fig. 12B). In contrast, the sample from Morel (M-1) has little slab influence and lies within the mantle array.

Figures 12A and 12B also show that the sources of Cretaceous volcanics arc rocks from Los Pasos Fm (Central Cuba), Maimón Fm (Central Cordillera, Dominican Republic), Puerto Rican volcanic phase I, and Paleogene volcanics rocks of El Cobre Group (SE Cuba) were depleted or N-MORB-type mantle wedges (Fig. 12B), without any evidence of contribution from an enriched mantle (e.g. mantle plume influence).

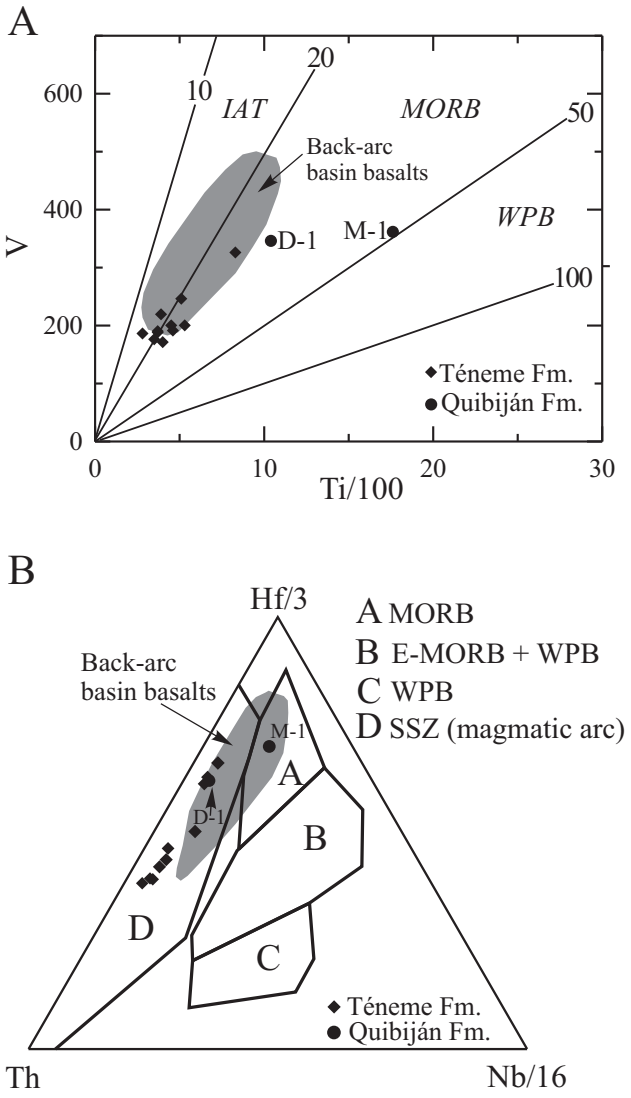

FIGURE 10 | **A) Ti/100 versus V discrimination diagram (Shervais, 1982) for basaltic rocks from the Téneme and Quibiján volcanic rocks. Back-arc field is from Metzger et al. (2002). B) Th-Hf/3-Nb/16 discrimination diagram (Wood, 1980) for the Téneme and Quibiján volcanic rocks. Back-arc and forearc basalts also plot within the SSZ field. Field for back-arc basin basalts is from compilation by Metzger et al. (2002).**

THE RÍO GRANDE INTRUSIVE

Geochemistry

The Río Grande quartz diorite consists of plagioclase, hornblende, deformed quartz, and minor biotite grains. K- feldspar is absent in all the analyzed samples. Commonly, these intrusive rocks show extensive albitization and sericitization of plagioclase and minor replacement of hornblende by chlorite and tremolite.

Geochemical data for the Rio Grande intrusive rocks are listed in Table 3. The SiO_2 content ranges from 58 to 60 wt%, and the MgO content varies between 2.34 and 2.65 wt%. All the samples are low in titanium ($TiO_2 \leq$ 0.47 wt%), potassium ($K_2O \leq$0.63 wt%), Y ($\leq$15 ppm), Yb ($\leq$1.5 ppm), and Nb ($\leq$1.6 ppm). On the Nb vs Y discrimination diagram (Pearce et al., 1984), the Téneme intrusive rocks plot within the volcanic-arc and syn-collisional granites field (no shown), while the K-Na-Ca plot (Fig. 13A) shows that Río Grande plutonics fall into the fields of Aruba batholith (Aruba, Dutch Caribbean; White et al., 1999) and granitoid rocks of the Cordillera Central (Dominican Republic; Lidiak and Jolly, 1996; Lewis et al., 2002).

As regards the REE contents of the Río Grande diorites, all samples exhibit low incompatible element values and patterns characterized by a slight LREE enrichment with flat MREE and HREE segments (Fig. 13B). The Río Grande quartz-diorites are not significantly depleted in HREE, suggesting that garnet control is insignificant in the origin of these intrusive rocks. The REE patterns are similar (except for the positive Eu anomaly) to those of the tonalitic batholith exposed in Aruba (White et al., 1999) and to those of granitoid rocks of the Cordillera Central (Dominican Republic; Lewis et al., 2002) (Fig. 13C). Finally, multielemental diagrams for intrusive rocks show negative Nb anomalies, typical of arc volcanic suite. The overall geochemical signature of Río Grande intrusive rocks supports the origin of these rocks in a subduction-related environment.

$^{40}Ar/^{39}Ar$ step-heating geochronology

The $^{40}Ar/^{39}Ar$ step-heating data are listed in Table 4 and presented in age spectra and isochron diagrams in Fig. 14.

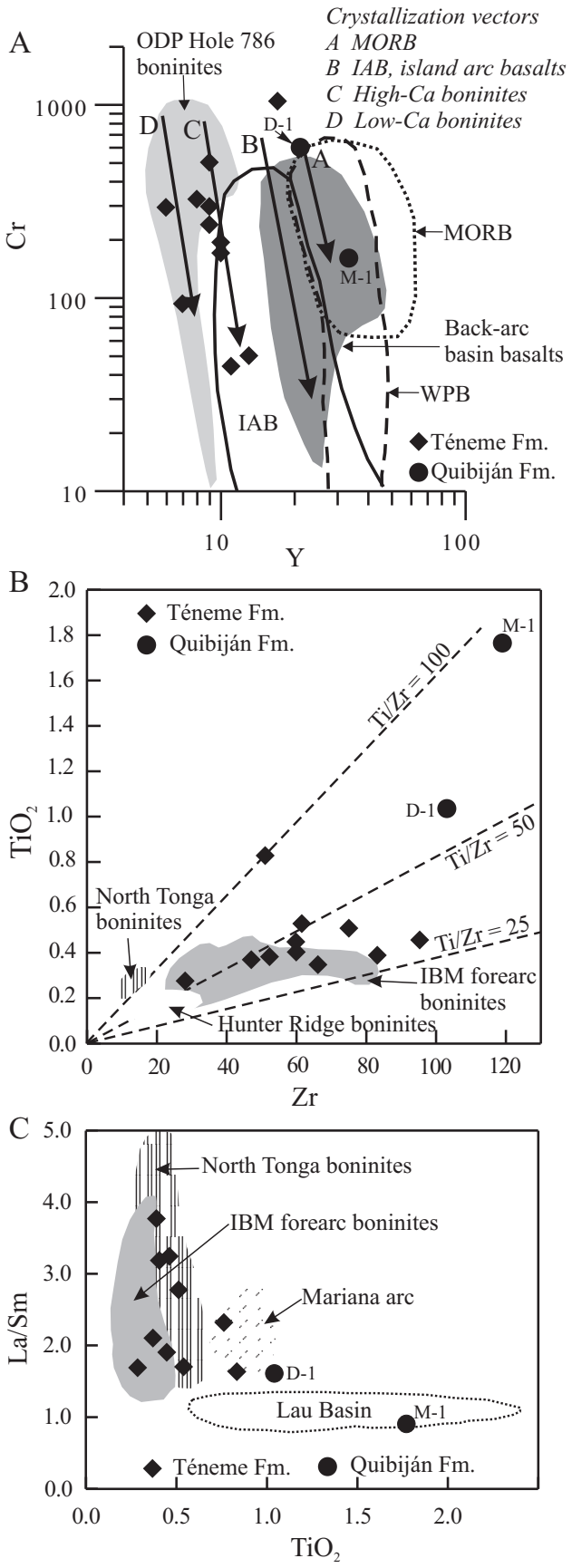

The age spectrum for hornblende sample Tm-37 (Fig. 14A) is fairly concordant but it does not form a plateau. However, the inverse-isotope correlation diagram (Fig. 14B) shows an isochron age at 89.70 ± 0.50 Ma with good statistical constraints ($^{40}Ar/^{36}Ar$ initial = 293 ± 6; MSWD = 1.6; 53.1% of total $^{39}Ar_K$ gas). A calculated average age at 89.40 ± 0.20 Ma supports the isochron age within limits of analytical error.

In contrast, hornblende sample Tm-35 presents a disturbed age spectrum (Fig. 14C) with a bad inverse-isotope correlation (unacceptable MSWD of 640; Fig. 14D). A calculated average age of 105.20 ± 0.30 Ma is the best approximation for the age of this hornblende sample; however, this age is clearly overestimating the age of the sample perhaps due to the presence of excess argon in the hornblende as observed in its climbing spectrum (Fig. 14C). This age is also too old based on geological field relationships since the package of Téneme volcanics, being intruded by the quartz diorite, present intercalated Cenomanian-Turonian fossil faunas (Iturralde-Vinent et al., this volume). This fact, combined with the relatively bad behaviour of this sample with respect to Argon systematics, force us to discard this analysis to determine the age of the quartz diorite.

The fine-grained, perhaps hypabissal(?) character of the quartz-diorite intrusion would imply that the cooling of the body was fairly fast, indicating that the hornblende isochron age at 89.70 ± 0.50 Ma (sample Tm-37) is the time of crystallization of the Rio Grande quartz diorite. In addition, this crystallization-intrusion age could be used to estimate the minimum possible age for the Téneme volcanics in the Rio Grande area.

DISCUSSION AND CONCLUSIONS

According to trace element discrimination diagrams presented in this paper, we infer that Téneme basaltic rocks are low-Ti island arc tholeiites (low-Ti IAT) with boninitic affinity. Two basalt samples from Quibiján Fm differ in their geochemical characteristics; e.g. Duaba basalt has a light REE enrichment normalized pattern, whereas Morel basalt has a relatively flat REE pattern similar to N-MORB. Thus, these volcanic rocks were not derived from the same parental magma, and should not be

FIGURE 11 | **A) Y-Cr discriminant diagram from Pearce et al. (1984) showing fields for basalts from various tectonic settings. Fields are from compilation by Metzger et al. (2002). B) Comparison of Zr and TiO_2 for Téneme and Quibiján volcanics and modern arc systems. Data for modern arc systems compilied by Meffre et al. (1996). C) Comparison of La/Sm and TiO_2 for the Téneme and Quibiján volcanics and modern arc systems. Data for modern arc system compiled by Meffre et al. (1996).**

included in the same lithostratigraphic unit (Quibiján Formation). These data indicate that the so-called Quibiján Formation, as defined today, include basalts from different origins, and in consequence need further detailed field, geochemical, and geochronological investigations.

The Téneme volcanic Formation consists of both tholeiites with boninitic affinity and typical oceanic arc tholeiites. These volcanic rocks have a geochemical signature similar to that of the Maimón Formation in Dominican Republic, (Lewis et al., 2000, 2001), and in general to that of the primitive (pre-Albian) island arc series described in the circum-Caribbean region.

Iturralde-Vinent et al. (this volume) propose, based on paleontological dating, a Turonian to early Coniacian age for Téneme Fm. This age is supported by the 89.70 ± 0.50 Ma Río Grande Instrusive that were probably emplaced during the final stages of arc magmatism. If this Late Cretaceous age is correct, primitive island arc volcanism in the Caribbean region was not extinguished in Aptian-Albian time (Donnelly and Rogers, 1980; Donnelly et al., 1990), but was still active in Late Cretaceous. In other words, Caribbean island arc development in Late Cretaceous (Albian-Campanian) is not only represented by

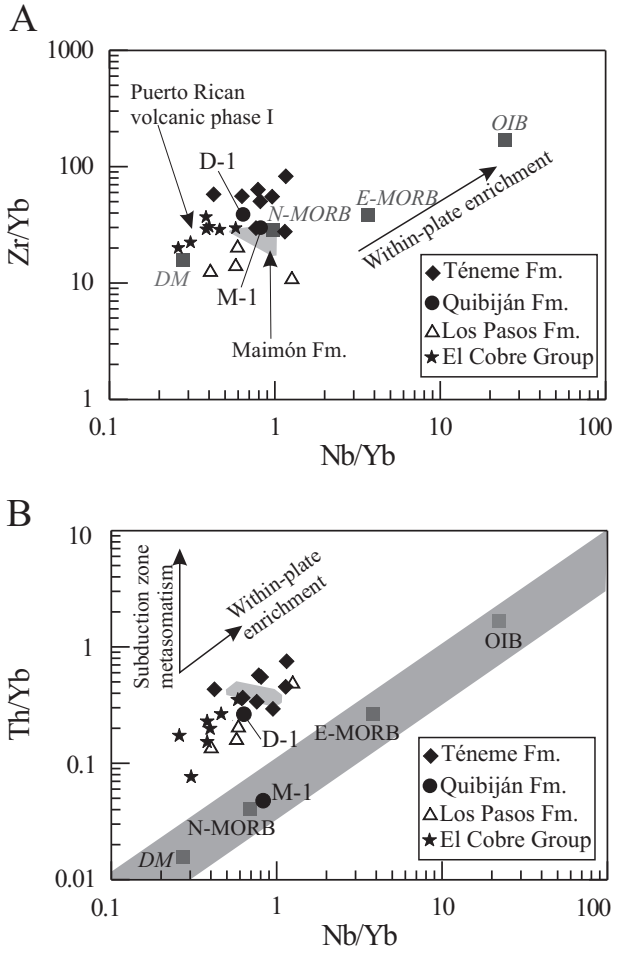

FIGURE 12 | **A) Zr/Yb versus Nb/Yb and (B) Th/Yb versus Nb/Yb plots for Téneme and Quibiján basaltic rocks. These diagrams (modified from Pearce and Peate, 1995) show the progression from depleted to enriched sources: DM = depleted mantle, from Staudigel et al. (1998); N-MORB, E-MORB and OIB from Sun and McDonough (1989). Geochemical analyses for Los Pasos (central Cuba) and El Cobre (eastern Cuba) basaltic rocks are from Proenza et al. (unpublished data). Field of Maimón Fm is taken from Lewis et al. (2000, 2002), and field form Puerto Rican volcanic phase I (Río Majada Group) is from Jolly et al. (2002).**

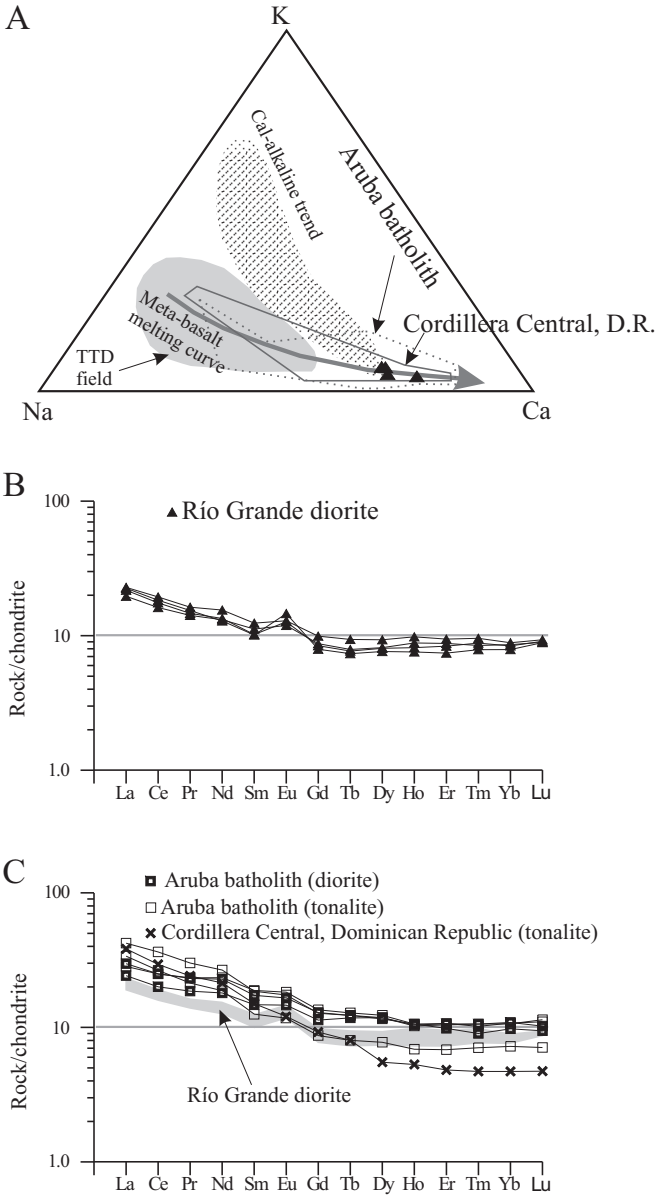

FIGURE 13 | **A) A) K-Na-Ca plot for the Río Grande intrusive rocks (after Defant and Drummond, 1993). Field for the Aruba batholith is from White et al. (1999), and the field for the Cordillera Central tonalite is from Lewis et al. (2002). B) Chondrite normalized (Sun and McDonough, 1989) REE patterns for the Río Grande intrusive. C) Río Grande intrusive rocks compared to diorites from Aruba batholith (White et al., 1999) and tonalite from Cordillera Central of Dominican Republic (Lewis et al., 2002).**

TABLE 4 | **$^{40}Ar/^{39}Ar$ step-heating data for quartz diorite samples Tm 35 and Tm-37 (Río Grande intrusive).**

Step	Temp. °C	%^{39}Ar of total	Radiogenic Yield (%)	$^{39}Ar_k$ (Moles x 10^{-12})	$^{40}Ar^*/^{39}Ar_k$	Apparent K/Ca	Apparent K/Cl	Apparent Age (Ma)	Error (Ma)
TM-37	***hornblende***	*J = 0.001981 ± 0.25%*		*wt = 110.0 mg*					
A	1000	0.8	19.3	0.000233	23.427	0.020	0.99	82.03	± 2.67
B	1025	1.0	30.7	0.000308	20.513	0.014	0.61	72.03	± 1.73
C	1050	1.8	42.0	0.000546	20.477	0.012	0.36	71.90	± 0.99
D	1075	3.2	57.0	0.000948	24.989	0.014	0.30	87.37	± 0.57
E	1100	6.7	69.2	0.001959	27.233	0.016	0.31	95.02	± 0.39
F	1125	12.6	76.3	0.003710	26.100	0.018	0.42	91.16	± 0.24
G	1150	20.6	83.3	0.006050	25.226	0.019	0.49	88.18	± 0.18
H	1175	7.0	80.2	0.002064	25.315	0.019	0.49	88.48	± 0.99
I	1200	3.1	73.8	0.000898	25.220	0.017	0.43	88.16	± 0.54
J	1225	2.6	66.7	0.000755	25.450	0.016	0.41	88.94	± 0.67
K	1250	4.3	77.8	0.001262	25.689	0.017	0.42	89.76	± 0.40
L	1275	11.2	82.4	0.003304	25.626	0.017	0.45	89.55	± 0.25
M	1300	11.9	82.3	0.003489	25.611	0.018	0.47	89.50	± 0.22
N	1350	10.0	78.4	0.002946	25.710	0.017	0.45	89.83	± 0.27
O	1450	3.0	68.9	0.000889	25.722	0.016	0.31	89.87	± 0.58
Total Gas								89.11	
86.4% of gas on plateau-like in 1125 through 1450 steps							**Average Age =**	**89.40**	**± 0.20**
TM-35	***hornblende***	*J = 0.001992 ± 0.25%*		*wt = 36.5 mg*					
A	1050	1.3	32.1	0.000168	20.874	0.017	0.71	73.67	± 2.80732
B	1100	5.6	60.9	0.000730	28.442	0.015	0.37	99.66	± 0.77932
C	1150	37.6	80.6	0.004913	28.371	0.019	0.47	99.41	± 0.24147
D	1200	14.8	81.4	0.001940	29.607	0.020	0.50	103.62	± 0.3513
E	1300	36.8	83.3	0.004828	31.810	0.018	0.47	111.10	± 0.22002
F	1450	3.9	62.9	0.000515	24.302	0.015	0.38	85.49	± 0.94684
Total Gas								103.50	
94.8% of gas on plateau-like in 1100 through 1300 steps							**Average Age =**	**105.20**	**± 0.30**

Ages calculated assuming an initial $^{40}Ar/^{36}Ar = 295.5\pm 0$.
All precision estimates are at the one sigma level of precision.
Ages of individual steps do not include error in the irradiation parameter J.
No error is calculated for the total gas age.

calc-alkaline (CA) volcanic rocks, as it has been suggested in previous studies (e.g. Donnelly et al., 1990; Lebron and Perfit, 1994; Kerr et al., 1999).

The geochemistry and age of Téneme volcanic rocks contrast with the Late Cretaceous geodynamic model of the Caribbean region, especially with respect to the position of the Caribbean oceanic plateau (Pindell and Barret, 1990). Mineral chemistry (e.g. very high Cr# values of Cr-spinel), and whole rock compositions (e.g. low Ti, Y, Nb abundances, and very low values of HREE) of Téneme basaltic rocks indicate a highly depleted mantle source for these magmas. The highly depleted mantle is likely to have been derived from previous melt extraction beneath the spreading ridge (Proto-Caribbean crust) and/or in a back-arc region related to Early Cretaceous island arc volcanism in the Greater Antilles. No contribution of E-MORB or OIB sources have been detected in the petrogenesis of the Téneme volcanics rocks. In contrast, the Late Cretaceous basement of the Dominican Republic Arc II (Lewis et al., 2002) displays an E-MORB signature. Such differences indicate that the volcanic rocks of eastern Cuba and the Dominican Republic were not segments of a single arc system in Upper Cretaceous. These results support a multiple-arc and oceanic microplates model for the Caribbean region in Upper Cretaceous time (Iturralde-Vinent, 2003).

Tholeiites with boninitic affinities, as Téneme volcanic rocks, are very rare in back-arc settings, whereas they are commonly generated during the initial stages of subduction in forearc regions (Stern et al., 1991; Pearce et al., 1992). In addition, Morel basaltic rocks exhibit a BABB affinity (Kerr et al., 1999; this study), and are partially coeval with Téneme volcanism (Iturralde-Vinent et al., this volume). Thus, the origin of Téneme and Morel volcanics from eastern Cuba can be explained in terms of a multistage process associated with an intra-oceanic subduction zone developed within the Caribbean region in Upper Cretaceous time. At this time, north-eastward-directed subduction

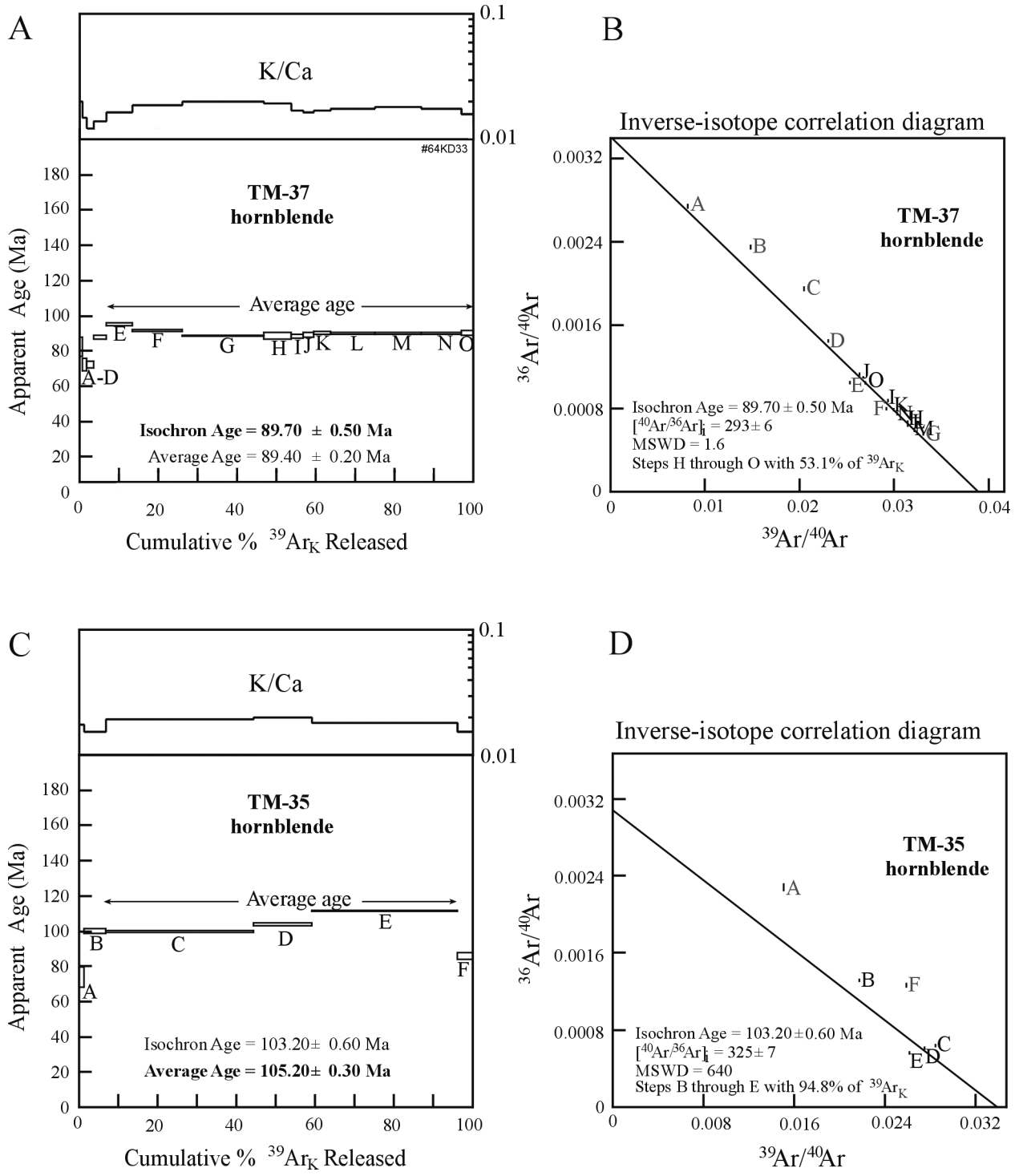

FIGURE 14 | **A) The $^{40}Ar/^{39}Ar$ age spectrum (A), and inverse-isotope correlation diagram (B) for hornblende sample Tm-37. The $^{40}Ar/^{39}Ar$ age spectrum (C), and inverse-isotope correlation diagram (D) for hornblende sample Tm-35.**

occurred beneath the Proto-Caribbean region, consuming Farallon plate (Kerr et al., 1999). Téneme volcanics were probably formed in a nascent primitive island arc, and therefore represent an example of forearc (or axial component) of this Upper Cretaceous IAT volcanism (PIA) recorded in eastern Cuba. In contrast, Morel volcanics probably were formed during extension of a back arc (or intra arc) basin, associated with the Téneme arc.

ACKNOWLEDGEMENTS

We are grateful to M. Iturralde-Vinent and J. Lewis for discussions and suggestions. Moreover we want to express our gratitude to E. Lidiak and an anonymous referee for critical reviewing and their constructive comments. We are very grateful to A. Camprubí, who provide support for the $^{40}Ar/^{39}Ar$ geochronology. Special thanks are given to X. Llovet for his assistance with electron-microprobe analysis. This paper was supported by AECI grant (Programa de Cooperación Científica con Iberoamérica) and the Spanish project BTE2001-3308, and is a contribution to IGCP Project 433 on Caribbean Plate Tectonics. We want to thank Mick Kunk for helping us with the $^{40}Ar/^{39}Ar$ geochronology. We also would like to thank Rebecca Morris for careful hornblende mineral separations.

REFERENCES

Adamovich, A.F., Chejovich, V.D., Trubino, D.Y., Shirikov, V.M., Pavlov, A.N., 1963. Estructura geológica y los minerales útiles de los macizos montañosos de Sierra de Nipe y Sierra Cristal, provincia de Oriente. Oficina Nacional de Recursos Minerales de Cuba, (unpublished).

Barnes, S.J., Roeder, P.L., 2001. The range of spinel compositions in terrestrial mafic and ultramafic rocks. Journal of Petrology, 42, 2279-2302.

Beccaluva, L., Macciotta, G., Piccardo, G.B., Zeda, O., 1989. Clinopyroxene compositions of ophiolites basalts as petrogenetic indicator. Chemical Geology, 77, 165-182.

Bortolotti, V., Marroni, M., Pandolfi, L., Principi, G., Saccani, E., 2002. Interaction between Mid-ocean ridge and subduction magmatism in Albanian Ophiolites. The Journal of Geology, 100, 561-576.

Blein, O., Guillot, S., Lapierre, H., Mercier de Lépinay, B., Lardeaux, J.M., Millan-Trujillo, G., Campos, M., Garcia, A., 2003. Geochemistry of the Mabujina Complex, Central Cuba: implications on the Cuban Cretaceous arc rocks. The Journal of Geology, 111, 89-101.

Cebula, G.T., Kunk, M.J., Mehnert, H.H., Naeser, C.W., Obradovich, J.D., Sutter, J.F., 1986. The Fish Canyon Tuff: A potential standard for the $^{40}Ar/^{39}Ar$ and fission track dating methods. Terra Cognita, 6, 2, p. 140.

Cobiella-Reguera, J.L., 2005. Emplacement of Cuban ophiolites. Geological Acta, 3, 273-294.

Defant, M.J., Drummond, M.S., 1993. Mount St. Helens: potential example of the partial melting of the subducted lithosphere in a volcanic arc. Geology, 21, 547-550.

Díaz de Villalvilla, L., 1997. Caracterización geológica de las formaciones volcano-sedimentarias en Cuba Central, provincias Cienfuegos, Villa Clara, Sancti Spiritus. In: Furrazola, G.F., Nuñez-Cambra, K.E. (eds.). Estudios sobre Geología de Cuba. Ciudad de la Habana, Cuba, Instituto de Geología y Paleontología, 325-344.

Díaz de Villalvilla, L., Pérez, M., Sukar, K., Marí, T., Méndez, I., Rodríguez, R., Piñero, R., Quintana, M.E., Aguirre, G., Echevarría, B., Milia, I., 1994. Consideraciones geoquímicas acerca de los arcos volcánicos de Cuba. Segundo Congreso Cubano de Geología y Minería. Libro de Programas y Resúmenes, Santiago de Cuba, p. 173.

Donnelly, T.W., Beets, D.J., Carr, M.J., Jackson, T., Kalver, G., Lewis, J., Maury, R., Schellekens, H., Smith, A., Wadge, G., Westercamp, D., 1990. History and tectonic setting of Caribbean magmatism. In: Dengo, G., Case, J.E. (eds.). The Caribbean. Decade of North American Geology, Boulder, Colorado, Geological Society of America, Volume H, 339-374.

Donnelly, T.W., Rogers, J.J.W., 1980. Igneous series in island arc: the northern Caribbean compared worldwide island arc assemblages. Bulletin of Volcanology, 43, 347-382.

Gyarmati, P., Leyé O'Conor, J., 1990. Informe final sobre los trabajos de levantamiento geológico en escala 1:50 000 y búsqueda acompañante en el polígono CAME V, Guantánamo. Oficina Nacional de Recursos Minerales, Cuba.

Gyarmati, P., Méndez, I., Lay, M., 1997. Caracterización de las rocas del arco de islas Cretácico en la Zona Estructuro-Facial Nipe-Cristal-Baracoa. In: Furrazola, G.F., Nuñez-Cambra, K.E (eds.). Estudios sobre Geología de Cuba. Ciudad de la Habana, Cuba, Instituto de Geología y Paleontología, 357-364.

Hawkesworth, C.J., Gallagher, K., Hergt, J.M., McDermott, F., 1993a. Mantle and slab contributions in arc magmas. Annual Reviews of Earth and Planetary Sciences, 21, 175-204.

Hawkesworth, C.J., Gallagher, K., Hergt, J.M., McDermott, F., 1993b. Trace elements fractionation processes in the generation of island arc basalts. Philosophical Transactions of the Royal Society of London, series A 342, 179-191.

Hawkins, J.W., Allan, J.F., 1994. Petrogenetic evolution of the Lau Basin sites 834 trough 839. Proceedings Ocean Drilling Program Scientific Results, 135, 427-470.

Iturralde-Vinent, M., 1976. Estratigrafía de la zona Calabazas-Achotal, Mayarí Arriba, Oriente. La Minería en Cuba, 5, 9-23.

Iturralde-Vinent, M., 1994. Cuban Geology: A new plate tectonic synthesis. Journal of Petroleum Geology, 17, 39-70.

Iturralde-Vinent, M., 1996a. Geología de las ofiolitas de Cuba. In: Iturralde-Vinent, M. (ed.). Ofiolitas y arcos volcánicos de Cuba. Miami, USA, IGCP Project 364, 83-120.

Iturralde-Vinent, M., 1996b. Cuba: el arco de islas volcánicas del Cretácico. In: Iturralde-Vinent, M. (ed.). Ofiolitas y arcos volcánicos de Cuba. Miami, USA, IGCP Project 364, 179-189.

Iturralde-Vinent, M., 1996c. Evidencias de un arco primitivo (Cretácico Inferior) en Cuba. In: Iturralde-Vinent, M. (ed.). Ofiolitas y arcos volcánicos de Cuba. Miami, USA, IGCP Project 364, 227-230.

Iturralde-Vinent, M.A., 2003. The relationship between the ophiolites, the metamorphic terrains, the Cretaceous volcanic arcs and the Paleocene-Eocene volcanic arc. Field guide to a geological excursion to Eastern Cuba. V Cuban Geological and Mining Congress. IGCP Project 433 Caribben Plate Tectonics. Cuban Geological Society, 16 pp.

Iturralde-Vinent, M., Díaz-Otero, C., Rodríguez-Vega, A., Díaz-Martínez, R., 2006. Tectonic implications of paleontologic dating of Cretaceous-Danian sections of Eastern Cuba. Geologica Acta, 4, 89-102.

Jolly, W.T., Lidiak, E.G., Dickin, A.P., Wu, T.W., 2001. Secular geochemistry of central Puerto Rican island arc lavas: constraints on Mesozoic tectonism in the Eastern Greater Antilles. Journal of Petrology, 42, 2197-2214.

Jolly, W.T., Lidiak, E.G., Dickin, A.P., Wu, T.W., 2002. Recycling in the Puerto Rican mantle wedge, Greater Antilles island arc. The Island Arc, 11, 10-24.

Kerr, A.C., Iturralde-Vinent, M., Saunders, A.D., Babbs, T.L., Tarney, J., 1999. A new plate tectonic model of the Caribbean: Implications from a geochemical reconnaissance of Cuban Mesozoic volcanic rocks. Geological Society of America Bulletin, 111, 1581-1599.

Knipper, A.L., Cabrera, R., 1974. Téctonica y geología histórica de la zona de articulación entre el mio- y eugeosinclinal y del cinturón hiperbasítico de Cuba. Academia de Ciencias de Cuba, Instituto de Geología, Contribución a la geología de Cuba, 15-77.

Kunk, M. J., Sutter, J. F., Naeser, C. W., 1985. High-precision $^{40}Ar/^{39}Ar$ Ages of Sanidine, Biotite, Hornblende, and Plagioclase from the Fish Canyon Tuff, San Juan Volcanic Field, South-central Colorado. Geological Society of America Abstracts with Programs, 17, p. 636.

Kunk, M. J., Winick, J. A., Stanley, J.O., 2001. $^{40}Ar/^{39}Ar$ age-spectrum and laser fusion data for volcanic rocks in west central Colorado. U.S. Geological Survey, Open-File Report 01-472, 94, pp.

Lebron, M.C., Perfit, M.R., 1993. Stratigraphic and petrochemical data support subduction polarity reversal of the Cretaceous Caribbean Island Arc. The Journal of Geology, 101, 389-396.

Lebron, M.C., Perfit, M.R., 1994. Chemistry and tectonic significance of Cretaceous island-arc rocks, Cordillera Oriental, Dominican Republic. Tectonophysics, 229, 69-100.

Leterrier, J., Maury, R.C., Thonon, P., Girard, D., Marchal, M., 1982. Clinopyroxene composition as a method of identification of the magmatic affinities of paleo-volcanic series. Earth Planetary Science Letters, 59, 139-154.

Lewis, J.F., Astacio, V.A., Espaillat, J., Jimenez, J., 2000. The occurrence of volcanogenic massive sulphide deposits in the Maimón Formation, Dominican Republic: The Cerro de Maimón, Loma Pesada and Loma Barbuito deposits. In: Sherlock, R. Barsch, R. Logan, A. (eds.). VMS deposits of Latin America. Geological Society of Canada Special Publication, 223-249.

Lewis, J.F., Escuder-Viruete, J., Hernaiz-Huerta, P.P., Gutiérrez, G., Draper, G., Pérez-Estaún, A., 2002. Subdivisión geoquímica del arco de Isla Circum-Caribeño, Cordillera Central Dominicana: Implicaciones para la formación, acreción y crecimiento cortical en un ambiente intraoceánico. Acta Geologica Hispanica, 37, 81-122.

Lewis, J.F., Perfit, M., Horan, S., Diaz de Villalvilla, L., 1995. Geochemistry and petrotectonic significance of early island arc bimodal volcanism in the Greater Antilles arc. Geological Society of America, Abstracts with Programs, New Orleans, Louisiana A-227.

Lidiak, E.G., Jolly, W.T., 1996. Circum-Caribbean granitoids: characteristics and origin. International Geology Review, 38, 1098-1133.

Lidiak, E.G., Jolly, W.T., 2002. Water Island Formation, U.S. Virgin Islands: a new look at the original primitive island arc (PIA) suite of the Caribbean. 16 Caribbean Geological Conference, Barbados, Abstracts, p. 34.

Linares, E., Osadchy, P., Dovbnia, A., et al., 1985. Mapa Geológico de la República de Cuba. Scale 1:50 000. Academia de Ciencias de Cuba. 4 sheets.

Marchesi, C., Proenza, J., Gervilla, F., Garrido, C.J., Melgarejo, J.C., Díaz-Martínez, R., Godard, M., 2003. New petrological and structural constraints on the origin of the Mayarí-Baracoa ophiolitic belt (eastern Cuba). Geophysical Research Abstracts, 5, 00278.

Marchesi, C., Garrido, C.J., Godard, M., Proenza, J.A., Gervilla, F., Blanco-Moreno, J., in press. Petrogenesis of highly depleted peridotites and gabbroic rocks from the Mayarí-Baracoa ophiolitic belts (eastern Cuba). Contributions to Mineralogy and Petrology.

Meffre, S., Aitchison, J.C., Crawford, A.J., 1996. Geochemical evolution and tectonic significance of boninites and tholeiites from Koh ophiolite, New Caledonia. Tectonics, 15, 67-83.

Metzger, E.P., Miller, R.B., Harper, G.D., 2002. Geochemistry and tectonic setting of the Ophiolitic Ingalls Complex, North Cascade, Washington: Implications for correlations of Jurassic Cordilleran Ophiolites. The Journal of Geology, 110, 543-560.

Morimoto, N., Fabries, J., Ferguson, A.K., Ginzburg, I.V., Ross, M., Seifeit, F.A., Zussman, J., 1989. Nomenclature of pyroxenes. Canadian Mineralogist, 27, 143-156.

Pearce, J., Lippard, S., Roberts, S., 1984. Characteristics and tectonic significance of supra-subduction zone ophiolites. Geological Society of London, Special Publication, 16, 77-94.

Pearce, J.A., Peate, D.W., 1995. Tectonic implications of the composition of volcanic arc magmas: Annual Reviews of Earth and Planetary Sciences, 23, 251-285.

Pearce, J.A., van der Laan, S.R., Arculus, R.J., Murton, B.J., Ishii, T., Peate, D.W., Parkinson, I.J., 1992. Boninite and harzburgite form Leg 125 (Bonin-Mariana forearc): A case study of magma genesis during the initial stages of subduction. Proceedings Ocean Drilling Program Science Results, 125, 623-659.

Pindell, J.L., Barrett, S.F., 1990. Geological evolution of the Caribbean region: a plate tectonic perspective. In: Dengo, G., Case, J.E. (eds.). The Caribbean. Decade of North American Geology, Boulder, Colorado, Geological Society of America, Volume H, 404-432.

Proenza, J., Gervilla, F., Melgarejo, J.C., Bodinier, J.L., 1999a. Al- and Cr- rich chromitites from the Mayarí-Baracoa Ophiolitic Belt (eastern Cuba): consequence of interaction between volatile-rich melts and peridotite in suprasubduction mantle. Economic Geology, 94, 547-566.

Proenza, J., Gervilla, F., Melgarejo, J.C., 1999b. La *Moho Transition Zone* en el Macizo Ofiolítico Moa-Baracoa: un ejemplo de interacción magma/peridotita. Revista de la Sociedad Geológica de España, 12, 309-327.

Proenza, J.A., Melgarejo, J.C., Gervilla, F., Rodríguez-Vega, A., Díaz-Martínez, R., Ruiz-Sánchez, R., Lavaut, W., 2003. Coexistence of Cr- and Al-rich ophiolitic chromitites in a small area: the Sagua de Tánamo district, Eastern Cuba. In: Eliopoulos et al. (eds.). Mineral Exploration and Sustainable Development. Rotterdam Netherlands, Millpress, 1, 631-634.

Pushcharovsky, Yu. et al., 1988. Geologic Map of the Republic of Cuba, Scale 1:250 000. Moscow. Cuban and USSR Academy of Sciences, 42 sheets.

Quintas, F., 1988. Características estratigráficas y estructurales del complejo ofiolítico y eugeosinclinal de la cuenca del Río Quibiján, Baracoa. Minería y Geología, 6, 11-22.

Quintas, F., 1989. Análisis estratigráfico y paleogeografía del Cretácico superior y del Paleógeno de la provincia de Guantánamo y áreas cercanas. Doctoral thesis. Instituto Superior Minero Metalúrgico de Moa., Holguín, Cuba, 161 pp.

Quintas, F., Hernández, M., Campos, M., 1994. Asociaciones estructuro-formacionales del Mesozoico en Cuba Oriental y La Española. Minería y Geología, 11, 3-9.

Shervais, J.W., 1982. Ti-V plots and the petrogenesis of modern and ophiolitic lavas. Earth Planetary Science Letters, 59, 101-118.

Simon, G., Kesler, S., Russel, N., Hall, C.M., Bell, D., Piñero, E., 1999. Epithermal gold mineralization in an old volcanic arc: the Jacinto deposit, Camagüey district, Cuba. Economic Geology, 94, 487-506.

Staudigel, H., Albarede, F., Blichert-Toft, J., Edmond, J., McDonough, W.F., Jacobsen, S.B., Keeling, R., Langmuir, C.H., Nielsen, R.L., Plank, T., Rudnick, R., Shaw, H.F., Shirey, S.B., Veizer, J., White, W., 1998. Geochemical Earth Reference Model GERM: description of the initiative. Chemical Geology, 145, 153-159.

Steiger, R. H., Jager, E., 1977. Subcommission on geochronology: Convention on the use of decay constants in geo- and cosmochronology. Earth and Planetary Science Letters, 36, 359-363.

Stern, R.J., Morris, J., Bloomer, S.H., Hawkins, J.W., 1991. The source of the subduction component in convergent margin magmas: trace element and radiogenic isotope evidence from Eocene boninites, Mariana forearc. Geochimica et Cosmochimica Acta, 55, 1467-1481.

Sun, S.-S., McDonough, W.F., 1989. Chemical and isotopic systematics of oceanic basalts: implications for mantle composition and processes. In: Saunder, A.D., Norry, M.J. (eds.). Magmatism in the ocean basins. Geological Society Special Publication, 42, 313-345.

Torrez, M., Fonseca, E., 1990. Características geológicas petrológicas del contacto entre la asociación ofiolítica y el arco volcánico en Moa-Baracoa. Boletín de Geociencias, Centro Universitario de Pinar del Río, Cuba, 1, 12-19.

White, R.V., Tarney, J., Kerr, A.C., Saunders, A.D., Kempton, P.D., Pringle, M.S., Klaver, G.T., 1999. Modification of an oceanic plateu, Aruba, Dutch Caribbean: implications for the generation of continental crust. Lithos, 46, 43-68.

Wood, D.A., 1980. The application of a Th-Hf-Ta diagram to problems of tectonomagmatic classification and to establishing the nature of crustal contamination of basaltic lavas of the Bristish Tertiary volcanic province. Earth and Planetary Science Letters, 50, 11-30.

Manuscript received October 2004;
revision accepted September 2005.